Electronic Supplementary Information

Same data, different structures: diastereoisomers with substantially identical NMR data from nature

Chuan-Xi Wang,[‡a] Guo-Dong Chen,[‡a] Chun-Chi Feng,[a] Rong-Rong He,[a] Sheng-Ying Qin,[b] Dan Hu,[a] He-Ru Chen,[a] Xing-Zhong Liu,[c] Xin-Sheng Yao,*[a] and Hao Gao*[a]

[a] Institute of Traditional Chinese Medicine & Natural Products, College of Pharmacy, Jinan University, Guangzhou 510632, People's Republic of China

[b] Clinical Experimental Center, First Affiliated Hospital of Jinan University, Guangzhou 510632, People's Republic of China

[c] State Key Laboratory of Mycology, Institute of Microbiology, Chinese Academy of Sciences, Beijing 100190, People's Republic of China

Corresponding author: Tel.: +86 20 8522 1559; fax: +86 20 8522 1559

Email address: tghao@jnu.edu.cn; tyaoxs@jnu.edu.cn

Table of Contents

1. NMR data assignments/comparisons of 1-4

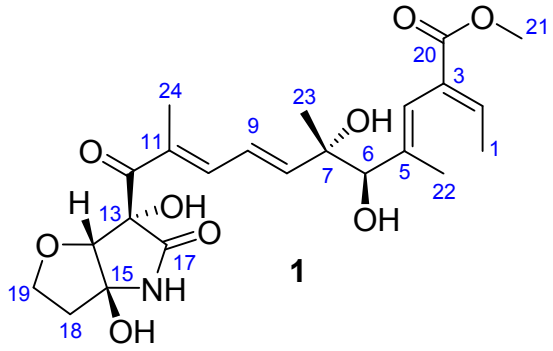

1

Table S1 NMR data of **1** in DMSO-d_6 (400 MHz for ^{1}H; 100 MHz for ^{13}C)

Position	δ_C, mult.	δ_H (J in Hz)	^{1}H,^{1}H-COSY	HMBC	ROESY
1	15.4, CH_3	1.67, br d (7.2)	2, 4	2, 3	22
2	138.8, CH	6.79, q (7.2)	1	1, 3, 4, 20	
3	130.0, qC	-			
4	119.9, CH	5.88, br s	1, 6, 22	2, 5, 6, 20, 22	6
5	141.4, qC	-			
6	81.4, CH	3.91, br d (4.9)	4, OH-6	4, 5, 7, 8, 22, 23	4, 8, 23
7	75.1, qC	-			
8	148.5, CH	6.27, d (15.2)	9	7, 10, 23	6, 10, 22
9	123.0, CH	6.59, dd (15.2, 11.7)	8, 10	7, 10, 11	OH-7, 23, 24
10	140.1, CH	7.22, br d (11.7)	9, 24	8, 12, 24	8, 14
11	132.1, qC	-			
12	198.9, qC	-			
13	85.1, qC	-			
14	91.8, CH	4.10, s	16	13, 15, 17, 19	10, OH-15, 18a, 19a, 24
15	93.2, qC	-			
16		8.64, br s	14	13, 14, 17	18b
17	173.0, qC	-			
18	38.6, CH_2	2.02, ddd (12.2, 6.0, 4.2), Ha	18b, 19a, 19b	15, 19	14
		1.96, ddd (12.2, 9.2, 7.1), Hb	18a, 19a, 19b	15, 19	16
19	67.7, CH_2	3.77, ddd (9.0, 7.1, 4.2), Ha	18a, 18b, 19b	14, 15	14
		3.49, ddd (9.2, 9.0, 6.0), Hb	18a, 18b, 19a	14, 15	
20	167.0, qC	-			
21	51.5, CH_3	3.64, s		20	
22	15.6, CH_3	1.47, br s	4	4, 5, 6	1, OH-6, OH-7, 8
23	25.7, CH_3	1.23, s		6, 7, 8	6, OH-6, 9
24	12.1, CH_3	1.80, br s	10	10, 11, 12	9, 14
OH-6		5.09, d (4.9)	6		22, 23
OH-7		4.66, br s		6, 7, 8, 23	9, 22
OH-13		6.63, br s		12, 14	
OH-15		6.23, br s		15, 18	14

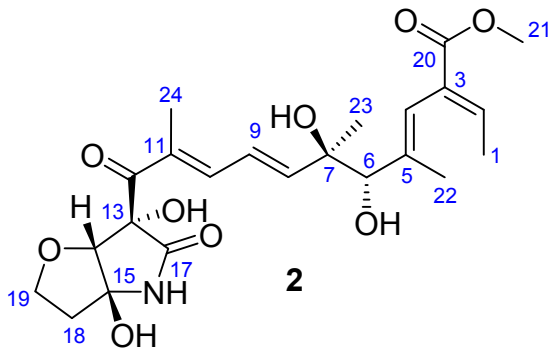

2

Table S2 NMR data of **2** in DMSO-d_6 (400 MHz for ^{1}H; 100 MHz for ^{13}C)

Position	δ_C, mult.	δ_H (*J* in Hz)	^{1}H,^{1}H-COSY	HMBC	ROESY
1	15.4, CH_3	1.67, br d (7.2)	2, 4	2, 3	22
2	138.9, CH	6.79, q (7.2)	1	1, 4, 20	
3	130.0, qC	-			
4	119.9, CH	5.87, br s	1, 6, 22	2, 5, 6, 20, 22	6, 23
5	141.5, qC	-			
6	81.4, CH	3.91, br d (5.0)	4, OH-6	4, 5, 7, 8, 22, 23	4, 8, 23
7	75.2, qC	-			
8	148.5, CH	6.27, d (15.2)	9	7, 10, 23	6, 10, 22
9	123.0, CH	6.59, dd (15.2, 11.7)	8, 10	7, 10, 11	23, 24
10	140.2, CH	7.22, br d (11.7)	9, 24	8, 12, 24	8, 14
11	132.0, qC	-			
12	199.0, qC	-			
13	85.2, qC	-			
14	91.8, CH	4.09, br s	16	13, 15, 17, 19	10, OH-15, 18a, 19a, 24
15	93.2, qC	-			
16		8.65, brs	14	13, 14, 17	18b
17	173.1, qC	-			
18	38.6, CH_2	2.02, ddd (12.2, 6.0, 4.2), Ha	18b, 19a, 19b	15, 19	14
		1.96, ddd (12.2, 9.2, 7.1), Hb	18a, 19a, 19b	15, 19	16
19	67.7, CH_2	3.77, ddd (9.0, 7.1, 4.2), Ha	18a, 18b, 19b	14, 15	14
		3.49, ddd (9.2, 9.0, 6.0), Hb	18a, 18b, 19a	14, 15	
20	167.0, qC	-			
21	51.5, CH_3	3.64, s		20	
22	15.6, CH_3	1.46, br s	4	4, 5, 6	1, 8
23	25.7, CH_3	1.23, s		6, 7, 8	4, 6, OH-6, 9
24	12.1, CH_3	1.80, br s	10	10, 11, 12	9, 14
OH-6		5.10, d (5.0)	6		23
OH-7		4.69, br s			
OH-13		6.70, br s			
OH-15		6.28, br s			14

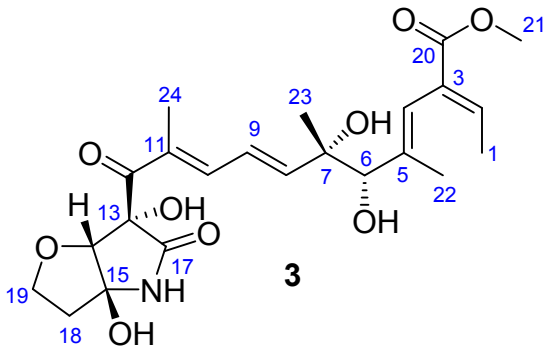

3

Table S3 NMR data of **3** in DMSO-d_6 (400 MHz for ^{1}H; 100 MHz for ^{13}C)

Position	δ_C, mult.	δ_H (*J* in Hz)	^{1}H,^{1}H-COSY	HMBC	ROESY
1	15.5, CH_3	1.65, br d (7.2)	2, 4	2, 3	22
2	139.0, CH	6.78, q (7.2)	1	1, 4, 20	
3	130.1, qC	-			
4	119.9, CH	5.91, br s	1, 6, 22	2, 5, 6, 20, 22	6, 23
5	141.7, qC	-			
6	80.7, CH	3.90, br d (5.1)	4, OH-6	4, 5, 7, 8, 22, 23	4, 8, 23
7	75.2, qC	-			
8	148.5, CH	6.28, d (15.2)	9	7, 10, 23	6, OH-6, 10
9	122.7, CH	6.58, dd (15.2, 11.7)	8, 10	7, 10, 11	24
10	140.2, CH	7.21, br d (11.7)	9, 24	8, 12, 24	8, 14
11	132.2, qC	-			
12	198.9, qC	-			
13	85.1, qC	-			
14	91.8, CH	4.10, br s	16	13, 15, 17, 19	10, OH-15, 18a, 19a, 24
15	93.3, qC	-			
16		8.65, br s	14	13, 14, 17	18b
17	173.1, qC	-			
18	38.7, CH_2	2.02, ddd (12.2, 6.0, 4.2), Ha	18b, 19a, 19b	15, 19	14
		1.96, ddd (12.2, 9.2, 7.1), Hb	18a, 19a, 19b	15, 19	16
19	67.7, CH_2	3.76, ddd (9.0, 7.1, 4.2), Ha	18a, 18b, 19b	14, 15	14
		3.49, ddd (9.2, 9.0, 6.0), Hb	18a, 18b, 19a	14, 15	
20	167.1, qC	-			
21	51.5, CH_3	3.63, s		20	
22	15.9, CH_3	1.48, br s	4	4, 5, 6	1, OH-6, OH-7
23	24.5, CH_3	1.22, s		6, 7, 8	4, 6
24	12.2, CH_3	1.80, br s	10	10, 11, 12	9, 14
OH-6		5.09, d (5.1)	6		8, 22
OH-7		4.71, br s			22
OH-13		6.66, br s		12, 14	
OH-15		6.25, br s			14

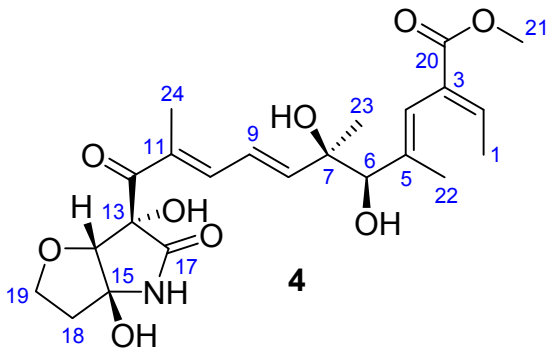

Table S4 NMR data of **4** in DMSO-d_6 (400 MHz for ^{1}H; 100 MHz for ^{13}C)

Position	δ_C, mult.	δ_H (J in Hz)	^{1}H,^{1}H-COSY	HMBC	ROESY
1	15.4, CH_3	1.64, br d (7.2)	2, 4	2, 3	22
2	139.0, CH	6.78, q (7.2)	1	1, 4, 20	
3	130.0, qC	-			
4	119.9, CH	5.91, br s	1, 6, 22	2, 5, 6, 20, 22	6, 23
5	141.7, qC	-			
6	80.7, CH	3.90, br d (5.1)	4, OH-6	4, 5, 7, 8, 22, 23	4, 8, 23
7	75.1, qC	-			
8	148.5, CH	6.28, d (15.2)	9	7, 10, 23	6, 10, 23, OH-6
9	122.7, CH	6.59, dd (15.2, 11.7)	8, 10	7, 10, 11	OH-7, 24
10	140.3, CH	7.22, br d (11.7)	9, 24	8, 12, 24	8, 14
11	132.2, qC	-			
12	198.9, qC	-			
13	85.2, qC	-			
14	91.8, CH	4.09, br s	16	13, 15, 17, 19	10, OH-15, 18a, 19a, 24
15	93.3, qC	-			
16		8.65, br s	14	13, 14, 17	18b
17	173.1, qC	-			
18	38.7, CH_2	2.02, ddd (12.2, 6.0, 4.2), Ha	18b, 19a, 19b	15, 19	14
		1.96, ddd (12.2, 9.2, 7.1), Hb	18a, 19a, 19b	15, 19	16
19	67.7, CH_2	3.76, ddd (9.0, 7.1, 4.2), Ha	18a, 18b, 19b	14, 15	14
		3.49, ddd (9.2, 9.0, 6.0), Hb	18a, 18b, 19a	14, 15	
20	167.1, qC	-			
21	51.5, CH_3	3.63, s			
22	15.8, CH_3	1.47, br s	4	4, 5, 6	1, OH-6, OH-7
23	24.6, CH_3	1.22, s		6, 7, 8	4, 6, 8
24	12.2, CH_3	1.80, br s	10	10, 11, 12	9, 14
OH-6		5.09, d (5.1)	6		8, 22
OH-7		4.71, br s			9, 22
OH-13		6.69, br s		12, 14	
OH-15		6.25, br s			14

Fusarin G1 (1): Yellowish oil; [α]15 D–37.9 (*c* 1.0, MeOH); UV (MeOH) λ_{max} (log ε): 207 (4.35), 287 (4.64) nm; CD (*c* 0.6 × 10^{-4} M, MeOH) λ_{max} ($\Delta\varepsilon$) 230 (+2.27), 289 (–5.97) 338 (+2.39); ESI-MS (positive) *m/z* 488.2 [M + Na]$^+$; HRESI-TOF-MS (positive): *m/z* 488.1901 [M + Na]$^+$ (calcd for $C_{23}H_{31}NO_9Na$, 488.1897); For the ^1H and ^{13}C NMR data, see Table S1.

Fusarin G2 (2): Yellowish oil; [α]15 D–84.8 (*c* 1.0, MeOH); UV (MeOH) λ_{max} (log ε): 207 (4.29), 287 (4.57) nm; CD (*c* 0.7 × 10^{-4} M, MeOH) λ_{max} ($\Delta\varepsilon$) 238 (–0.46), 288 (–5.53) 338 (+2.39); ESI-MS (positive) *m/z* 488.2 [M + Na]$^+$; HRESI-TOF-MS (positive): *m/z* 488.1889 [M + Na]$^+$ (calcd for $C_{23}H_{31}NO_9Na$, 488.1897); For the ^1H and ^{13}C NMR data, see Table S2.

Fusarin G3 (3): Yellowish oil; [α]15 D–83.9 (*c* 1.0, MeOH); UV (MeOH) λ_{max} (log ε): 207 (4.39), 287 (4.64) nm; CD (*c* 0.6 × 10^{-4} M, MeOH) λ_{max} ($\Delta\varepsilon$) 238 (+1.34), 289 (–6.33), 339 (+2.40); ESI-MS (positive) *m/z* 488.2 [M + Na]$^+$; HRESI-TOF-MS (positive): *m/z* 488.1891 [M + Na]$^+$ (calcd for $C_{23}H_{31}NO_9Na$, 488.1897); For the ^1H and ^{13}C NMR data, see Table S3.

Fusarin G4 (4): Yellowish oil; [α]15 D–50.4 (*c* 1.0, MeOH); UV (MeOH) λ_{max} (log ε): 207 (4.23), 287 (4.43) nm; CD (*c* 0.9 × 10^{-4} M, MeOH) λ_{max} ($\Delta\varepsilon$) 230 (–1.12), 287 (–4.10), 343 (+2.50); ESI-MS (positive) *m/z* 488.2 [M + Na]$^+$; HRESI-TOF-MS (positive): *m/z* 488.1893 [M + Na]$^+$ (calcd for $C_{23}H_{31}NO_9Na$, 488.1897); For the ^1H and ^{13}C NMR data, see Table S4.

Table S5. The comparisons in chemical shifts between **1** and **2**, between **3** and **4**, between **1** and **3**. (400 MHz for ^{1}H; 100 MHz for ^{13}C; in DMSO-d_6; $\Delta\delta$ in ppm)

	$\Delta\delta$ (**1**-**2**)		$\Delta\delta$ (**3**-**4**)		$\Delta\delta$ (**1**-**3**)	
No.	$\lvert\Delta\delta_H\rvert$	$\lvert\Delta\delta_C\rvert$	$\lvert\Delta\delta_H\rvert$	$\lvert\Delta\delta_C\rvert$	$\lvert\Delta\delta_H\rvert$	$\lvert\Delta\delta_C\rvert$
1	0.00	0.0	0.01	0.1	0.02	0.1
2	0.00	0.1	0.00	0.0	0.01	0.2
3	-	0.0	-	0.1	-	0.1
4	0.01	0.0	0.00	0.0	0.03	0.0
5	-	0.1	-	0.0	-	0.3
6	0.00	0.0	0.00	0.0	0.01	0.7
7	-	0.1	-	0.1	-	0.1
8	0.00	0.0	0.00	0.0	0.01	0.0
9	0.00	0.0	0.01	0.0	0.01	0.3
10	0.00	0.1	0.01	0.1	0.01	0.1
11	-	0.1	-	0.0	-	0.1
12	-	0.1	-	0.0	-	0.0
13	-	0.1	-	0.1	-	0.0
14	0.01	0.0	0.01	0.0	0.00	0.0
15	-	0.0	-	0.0	-	0.1
16	0.01	-	0.00	-	0.01	-
17	-	0.1	-	0.0	-	0.1
18	0.00	0.0	0.00	0.0	0.00	0.1
	0.00	-	0.00	-	0.00	-
19	0.00	0.0	0.00	0.0	0.01	0.0
	0.00	-	0.00	-	0.00	-
20	-	0.0	-	0.0	-	0.1
21	0.00	0.0	0.00	0.0	0.01	0.0
22	0.01	0.0	0.01	0.1	0.01	0.3
23	0.00	0.0	0.00	0.1	0.01	1.2
24	0.00	0.0	0.00	0.0	0.00	0.1
O<u>H</u>-6	0.01	-	0.00	-	0.00	-
O<u>H</u>-7	0.03	-	0.00	-	0.05	-
O<u>H</u>-13	0.07	-	0.03	-	0.03	-
O<u>H</u>-15	0.05	-	0.01	-	0.02	-

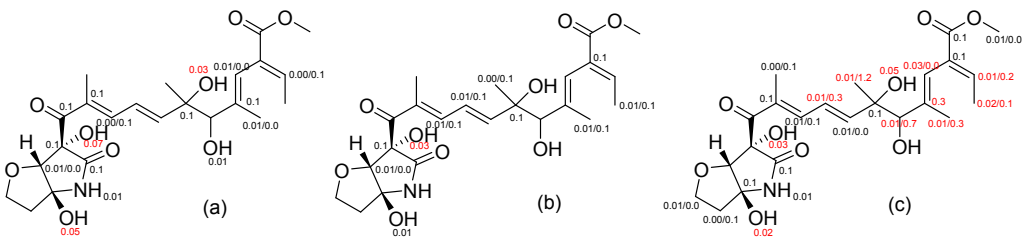

Figure S1. The differences in chemical shifts

(a): between **1** and **2**, (b): between **3** and **4**, (c): between **1** and **3**

2. Experimental section

2.1 General experimental procedures

Optical rotations were measured on a JASCO P1020 digital polarimeter, and UV data were recorded on a JASCO V-550 UV/vis spectrometer. CD spectra were recorded on a JASCO J-810 spectrophotometer using MeOH as the solvent. ESI-MS spectra were performed on a Finnigan LCQ Advantage MAX spectrometer and HR-ESI MS spectra were obtained on Waters Synapt G2 mass spectrometer. ^{1}H and ^{13}C NMR spectra were acquired with Bruker AV 400 and AV 600 spectrometers using solvent signals (DMSO-d_6: δ_H 2.50/δ_C 39.5, pyridine-d_5: δ_H 7.21/δ_C 123.5) as internal standards. Analytical HPLC was performed on a Dionex HPLC system equipped with an Ultimate 3000 pump, an Ultimate 3000 diode array detector (DAD), an Ultimate 3000 Column Compartment, an Ultimate 3000 autosampler (Dionex, USA) using a Phenomex Gemini C18 column (4.6 × 250 mm, 5 μm). Semi-preparative HPLC was carried out on a Dionex HPLC system equipped with an Ultimate 3000 pump, and an Ultimate 3000 RS variable wavelength Detector (Dionex, USA) using a Phenomex Gemini C18 column (10.0 × 250 mm, 5 μm). The medium-pressure liquid chromatography (MPLC) system was equipped with a dual pump gradient system, an UV preparative detector, and a Dr Flash II fraction collector system (Shanghai Lisui E-Tech Co., Ltd.). Column chromatography (CC) was carried out on ODS (50 μm, YMC). TLC was performed on precoated silica gel plates (SGF_{254}, 0.2 mm, Yantai Chemical Industry Research Institute, China).

2.2 Fungus materials and fermentation

The strain of *Mucor* sp. was isolated from soil collected in Sinkiang province, People's Republic of China. The isolate was identified by one of the authors (X. Z. Liu) and assigned the accession number XJ07015-2 in the culture collection at the Institute of Traditional Chinese Medicine and Natural Products, College of Pharmacy, Jinan University. The fungal strain was identified as *Mucor* sp. based on its morphological characteristics and analysis of the internal transcribed spacer (ITS) sequence. In brief, the ITS region of the fungal strain was amplified by PCR and sequenced. A blast search of the ITS sequence (Gene bank accession number: KP677280) showed a 99% sequence identity with *Mucor hiemalis* (Gene bank accession number: KF944455.1). The detailed identification method for the ITS sequence analysis is described below.

Fresh fungal mycelia (about 50 mg) were obtained by centrifuging 1 mL of fresh culture in a 1.5 mL micro-centrifuge tube. 100 μL of preheated (60 °C) 2 × CTAB extraction buffer (2% CTAB (w/v), 100 mM Tris-HCl, 1.4 M NaCl, 20 mM EDTA, pH 8.0) and 0.2 g sterilized quartz sand (Sangon Biotech Co., Ltd, Shanghai, China) were added, and the fungal mycelia were ground using a glass pestle. 500 μL of preheated (60 °C) 2 × CTAB extraction buffer was added, and incubated at 60 °C for 30 min with occasional gentle swirling. After that, 500 μL of phenol-chloroform (1:1, v/v) was added and mixed thoroughly to form an emulsion. The mixture was centrifuged at 10,000 rpm for 10 min at room temperature. The aqueous phase (500 μL) was removed, placed into a fresh 1.5 mL tube and extracted with 500 μL chloroform. The mixture was centrifuged at 10,000 rpm for 10 min at room temperature and the aqueous phase (400 μL) was transferred into a new 1.5 mL tube. Isopropanol (400 μL) was added and the genomic DNA in the aqueous phase was precipitated by centrifuging at 10,000 rpm for 10 min. The DNA pellet was washed with 70% ethanol twice, dried, and suspended in 50 μL H_2O. The primer pairs ITS1 (5'-TCCGTAGGTGAACCTGCGG-3') and ITS4 (5'-TCCTCCGCTTATTGATATGC-3') were used for amplification of the ITS fragment, which was performed using a TaKaRa PCR Amplification Kit (Takara, Dalian, China). After PCR, 4 μL of the reaction mixture was loaded onto an agarose gel (1% agarose) and subjected to electrophoresis. After the band containing the PCR products (approximate size 550 bp for the partial ITS gene) was confirmed, the PCR products were then submitted for sequencing (Sangon Biotech, Shanghai, China) with the corresponding primers. The sequence data have been submitted to GenBank.

The fungal strain was cultured on slants of potato dextrose agar (PDA) at 25 °C for 5 days. Agar plugs were used to inoculate four Erlenmeyer flasks (250 mL), each containing 100 mL of potato dextrose broth (PDB). The four flasks of the inoculated media were incubated at 25 °C on a rotary shaker at 200 rpm for five days to prepare the seed culture. Fermentation was carried out in twenty Erlenmeyer flasks (500 mL), each containing 70 g of rice. Distilled H_2O (105 mL) was added to each flask, and the rice was soaked overnight before autoclaving at 120 °C for 30 min. After cooling to room temperature, each flask was inoculated with 5.0 mL of the spore inoculum and incubated at 25 °C for 60 days.

2.3 Extraction and isolation

The fermented material was extracted twice with EtOAc, and the organic solvent was removed under reduced pressure to yield the crude extract (32.5 g). The crude extract was dissolved in 90% v/v aqueous MeOH (500 mL) and partitioned against the same volume of cyclohexane to afford a cyclohexane fraction (C, 15.2 g) and an aqueous MeOH fraction (W, 13.7 g). The aqueous MeOH fraction (W, 13.7 g) was separated by ODS CC (4 × 28 cm) with elution by MeOH–H_2O (30:70, 50:50, 70:30, 90:10 and 100:0, v/v, each 800 mL) to afford 5 fractions (W1–W5). Fraction W2 (3.6 g) was further separated by MPLC with gradient elution by MeOH-H_2O (15%–100%, v/v) to afford fourteen subfractions (W2a to W2n). Subfraction W2i (60.4 mg) was purified by semi-preparative HPLC, using MeOH–H_2O (50:50, v/v) at a flow rate of 1.5 mL/min to yield **1** (t_R: 26.1min, 29.5 mg). Subfraction W2g (99.9 mg) was purified by semi-preparative HPLC, using MeOH–H_2O (50:50, v/v) at a flow rate of 1.5 mL/min to yield **2** (t_R: 24.2 min, 22.0 mg). Subfraction W2e (232.8 mg) was purified by semi-preparative HPLC, using MeOH–H_2O (50:50, v/v) at a flow rate of 1.5 mL/min to yield **4** (t_R: 22.0 min, 23.8 mg) and **3** (t_R: 22.8 min, 10.6 mg). **1**-**4** were analysis by HPLC method under the same condition (Figure S2).

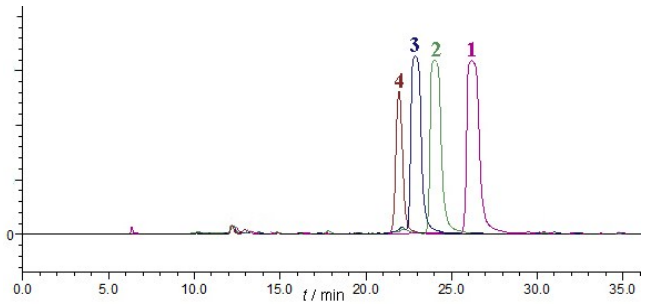

Figure S2. The HPLC chromatogram for **1**–**4** (Phenomex Gemini C18, 5 μm, 10 × 250 mm; MeOH/H_2O 50:50; flow rate 1.5 mL/min; 210 nm).

2.4 Catalytic hydrogenation of fusarins G1 (1) and G2 (2)

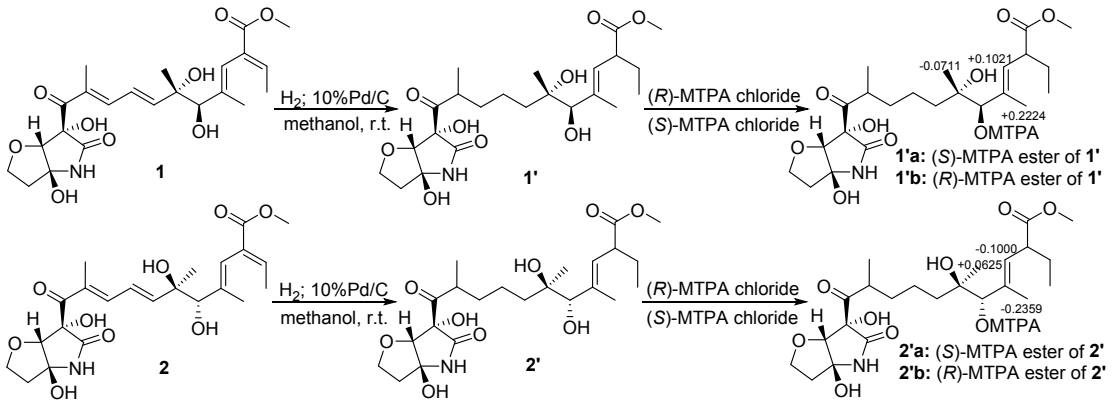

Scheme S1. Application of a modified Mosher's method after catalytic hydrogenation for determination of the absolute configuration of C-6 in **1** and **2** ($\Delta\delta$ ($\delta_S - \delta_R$) values (in ppm) obtained for (*S*)- and (*R*)-MTPA esters (**1'a** and **1'b**, **2'a** and **2'b**))

Fusarin G1 (**1**) (4 mg, 0.008 mmol) was dissolved in MeOH (2 mL) and reduced with 10% Pd/C (4 mg) under a H_2 atmosphere for 24 h at room temperature. The mixture was filtered, and the filtrate was evaporated and separated by semi-preparative HPLC (Phenomex Gemini C_{18}, 5 μm, 10 × 250 mm; gradient of 20% to 40% MeOH/H_2O in 30 min; flow rate 1.5 mL/min; 210 nm) to give **1'** (1 mg).

Fusarin G2 (**2**) (4 mg, 0.008 mmol) was dissolved in MeOH (2 mL) and reduced with 10% Pd/C (4 mg) under a H_2 atmosphere for 24 h at room temperature. The mixture was filtered, and the filtrate was evaporated and separated by semi-preparative HPLC (Phenomex Gemini C_{18}, 5 μm, 10 × 250 mm; gradient of 20% to 40% MeOH/H_2O in 30 min; flow rate 1.5 mL/min; 210 nm) to give **2'** (1 mg).

1': Amorphous powder; ^{1}H NMR (pyridine-d_5, 600 MHz) δ 0.89 (3H, t, J = 7.3 Hz, H_3-1), 1.86 (1H, m, Ha-2), 1.63 (1H, m, Hb-2), 3.45 (1H, dt, J = 9.4, 7.1 Hz, H-3), 5.69 (1H, br d, J = 9.6 Hz, H-4), 4.32 (1H, br s, H-6), 1.60-1.97 (6H, overlapped, H_2-8, H_2-9, H_2-10), 2.33 (1H, m, H-11), 4.96 (1H, br s, H-14), 2.51 (2H, m, H_2-18), 4.24 (1H, m, Ha-19), 4.13 (1H, m, Hb-19), 3.65 (3H, s, H_3-21), 2.10 (3H, br s, H_3-22), 1.40 (3H, s, H_3-23), 1.31 (3H, d, J = 6.8 Hz, H_3-24), 10.31 (1H, br s, exchangeable hydrogen), 9.02 (1H, br s, exchangeable hydrogen), 6.40 (1H, br s, O<u>H</u>-6), 5.65 (1H, br s, exchangeable hydrogen), 5.03 (1H, br s, exchangeable hydrogen). ESI-MS *m/z* 494.2 [M + Na]$^+$, *m/z* 470.7 [M - H]$^-$.

2': Amorphous powder; ^{1}H NMR (pyridine-d_5, 600 MHz) δ 0.89 (3H, t, J = 7.5 Hz, H_3-1), 1.86 (1H, m, Ha-2), 1.63 (1H, m, Hb-2), 3.45 (1H, dt, J = 9.5, 7.3 Hz, H-3), 5.69 (1H, br d, J = 9.5 Hz, H-4), 4.32 (1H, br s, H-6), 1.60-1.97 (6H, overlapped, H_2-8, H_2-9, H_2-10), 2.33 (1H, m, H-11), 4.96 (1H, br s, H-14), 2.51 (2H, m, H_2-18), 4.24 (1H, m, Ha-19), 4.13 (1H, m, Hb-19), 3.66 (3H, s, H_3-21), 2.09 (3H, br s, H_3-22), 1.39 (3H, s, H_3-23), 1.31 (3H, d, J = 6.6 Hz, H_3-24), 10.31 (1H, br s, exchangeable hydrogen), 9.03 (1H, br s, exchangeable hydrogen), 6.43 (1H, br s, O<u>H</u>-6), 5.66 (1H, br s, exchangeable hydrogen), 5.05 (1H, br s, exchangeable hydrogen). ESI-MS *m/z* 494.2 [M + Na]$^+$, *m/z* 470.8 [M - H]$^-$.

2.5 Preparation of (*S*) and (*R*) -MTPA esters (1'a/2'a and 1'b/2'b) of 1'/2'

A solution of **1'/2'** (0.5 mg) in pyridine-d_5 (0.5 mL) was treated with (*R*)-MTPA chloride (15 μL) under an atmosphere of nitrogen in an NMR tube. The mixture was placed at room temperature for 4 h to obtain the (*S*)-MTPA ester (**1'a/2'a**). The same procedure was used to prepare the (*R*)-MTPA ester (**1'b/2'b**) with (*S*)-MTPA chloride.

The key $\Delta\delta$ values ($\Delta\delta_{H\text{-}4}$: +0.1021; $\Delta\delta_{H\text{-}22}$: +0.2224; $\Delta\delta_{H\text{-}23}$: -0.0711) of the (*S*)- and (*R*)-MTPA esters of **1'** (**1'a** and **1'b**) indicated the *R* configuration for C-6 in **1**.

The key $\Delta\delta$ values ($\Delta\delta_{H\text{-}4}$: -0.1000; $\Delta\delta_{H\text{-}22}$: -0.2359; $\Delta\delta_{H\text{-}23}$: +0.0625) of the (*S*)- and (*R*)-MTPA esters of **2'** (**2'a** and **2'b**) indicated the *S* configuration for C-6 in **2**.

2.6 Ozonolysis of fusarins G1–G4 (1–4)

A solution of **1** (5.0 mg) in $CHCl_3/CH_3OH$ (1:1, 6 mL) was treated with O_3 at –78 °C for 30 min. After excess O_3 was removed by a stream of N_2, the reaction mixture was treated with dimethyl sulfide at room temperature for 12 hours. The residue, after evaporation, was separated by semi-preparative HPLC (Phenomex Gemini C18, 5 μm, 10 × 250 mm; $MeOH/H_2O$ 5:95; flow rate 1.5 mL/min; 210 nm) to afford **5** (2mg).

The same procedure was used for **2**-**4**. The products of **2**-**4** after the ozonolysis reaction was identified as **5** by the retention times, ^{1}H NMR data, and ECD spectra.

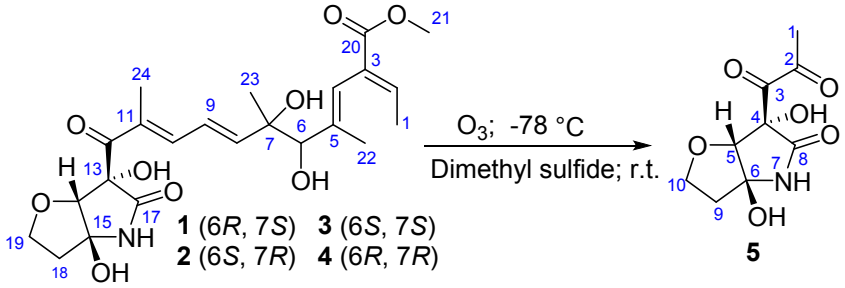

Scheme S2. **5** was obtained from **1**–**4** by the ozonolysis reaction respectively

5: Yellowish oil; [α]19 D–59.6 (*c* 0.5, MeOH); UV (MeOH) λ_{max} (log ε): 205 (3.65) nm; CD (*c* 4.7 × 10^{-4} M, MeOH) λ_{max} ($\Delta\varepsilon$) 216 (+1.77), 248 (–0.27), 274 (+0.60), 307 (–0.30); ESI-MS (positive) *m/z* 251.9 $[M + Na]^+$; ESI-MS (negative) *m/z* 227.9 $[M - H]^-$; HRESI-TOF-MS (positive): *m/z* 252.0483 $[M + Na]^+$ (calcd for $C_9H_{11}NO_6Na$, 252.0484); For the ^{1}H and ^{13}C NMR data, see Table S6.

Table S6 NMR data of **5** in DMSO-d_6 (600 MHz for ^{1}H; 150 MHz for ^{13}C)

Position	δ_C, mult.	δ_H (*J* in Hz)	^{1}H,^{1}H-COSY	HMBC
1	24.6, CH_3	2.22, s		2, 3
2	196.9, qC	-		
3	197.8, qC	-		
4	82.8, qC	-		
5	91.1, CH	3.99, s		3, 4, 6, 8, 10
6	93.3, qC	-		
7	-	8.95, s		4
8	170.6, qC	-		
9	38.2, CH_2	2.07, m	10a, 10b	6, 10
10	67.6, CH_2	3.81, ddd (14.0, 7.1, 4.7), Ha	9, 10b	6
		3.56, ddd (14.0, 7.9, 6.0), Hb	9, 10a	6
OH-4*	-	6.68, br s		
OH-6*	-	6.38, br s		

*Assignments can be exchanged with each other.

2.7 Quantum chemical ECD calculations of 5

The molecular structures of (4*R*, 5*R*, 6*S*)-**5** and (4*S*, 5*S*, 6*R*)-**5** were converted into SMILES code before their initial 3D structures were generated with CORINA version 3.4. For each molecule, the initial 3D structure was minimized with the MMFF94S force field implemented in CONFLEX version 7.0 with the default parameters before its conformation space was sampled. The conformer databases were generated using CONFLEX version 7.0, with an energy window for acceptable conformers (ewindow) of 5 kcal mol^{-1} above the ground state using the modified version of the MMFF94 force-field mentioned above, a maximum number of conformations per molecule (maxconfs) of 100 and an RMSD cutoff (rmsd) of 0.5Å. This resulted in only one conformer. Then the conformer was optimized with the HF/6-31G (d) method in Gaussian 09 (1). Further optimization at the B3P86/6-31G (d) level produced the dihedral angles. The optimized conformer was used for the ECD calculations, which were performed with Gaussian 09 (B3P86/6-311++G (2d, p)). The solvent effects were taken into account by the polarizable-conductor calculation model (CPCM, methanol as the solvent).

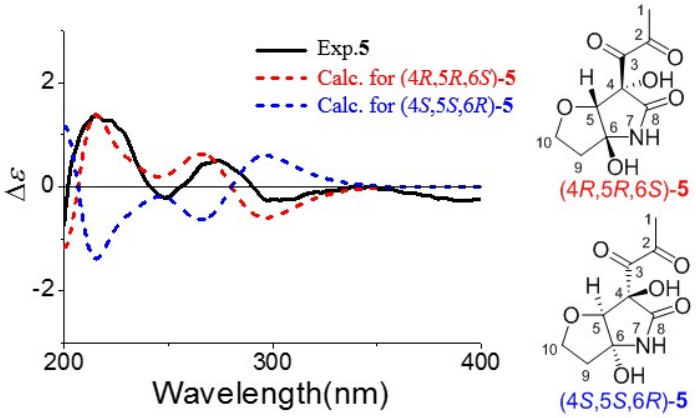

Figure S3. Experimental ECD spectrum of **5** and calculated CD spectra of (4*R*, 5*R*, 6*S*)-**5** and (4*S*, 5*S*, 6*R*)-**5** (UV correction = 0 nm, band width σ = 0.3 eV)

References:

(1) Frisch, M. J.; Trucks, G. W.; Schlegel, H. B.; Scuseria, G. E.; Robb, M. A.; Cheeseman, J. R.; Scalmani, G.; Barone, V.; Mennucci, B.; Petersson, G. A.; Nakatsuji, H.; Caricato, M.; Li, X.; Hratchian, H. P.; Izmaylov, A. F.; Bloino, J.; Zheng, G.; Sonnenberg, J. L.; Hada, M.; Ehara, M.; Toyota, K.; Fukuda, R.; Hasegawa, J.; Ishida, M.; Nakajima, T.; Honda, Y.; Kitao, O.; Nakai, H.; Vreven, T.; Montgomery, J. A., Jr.; Peralta, J. E.; Ogliaro, F.; Bearpark, M.; Heyd, J. J.; Brothers, E.; Kudin, K. N.; Staroverov, V. N.; Kobayashi, R.; Normand, J.; Raghavachari, K.; Rendell, A.; Burant, J. C.; Iyengar, S. S.; Tomasi, J.; Cossi, M.; Rega, N.; Millam, J. M.; Klene, M.; Knox, J. E.; Cross, J. B.; Bakken, V.; Adamo, C.; Jaramillo, J.; Gomperts, R.; Stratmann, R. E.; Yazyev, O.; Austin, A. J.; Cammi, R.; Pomelli, C.; Ochterski, J. W.; Martin, R. L.; Morokuma, K.; Zakrzewski, V. G.; Voth, G. A.; Salvador, P.; Dannenberg, J. J.; Dapprich, S.; Daniels, A. D.; Farkas, Ö.; Foresman, J. B.; Ortiz, J. V.; Cioslowski, J.; Fox, D. J. Gaussian 09, Revision C1; Gaussian, Inc., Wallingford CT, **2010**.

2.8 The *in situ* dimolybdenum CD method

HPLC grade DMSO was dried with 4Å molecular sieves. Following a previously published procedure (2), a mixture of 1:1.3 diol-$Mo_2(OAc)_4$ for **3** (or **4**) was subjected to CD measurement at a concentration of 0.5 mg/mL. The first CD spectrum was recorded immediately after mixing, and its time evolution was monitored until stationary (about 10 min after mixing). The inherent CD was subtracted. The observed signs of the diagnostic bands at around 310 nm in the induced CD spectrum were correlated to the absolute configuration of C-6 and C-7.

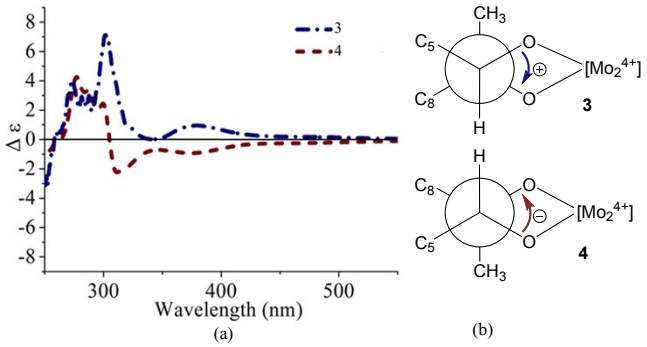

Figure S4. (a) The CD spectra of **3** and **4** in DMSO containing $Mo_2(OAc)_4$ with the inherent CD spectra subtracted; (b) Conformations of the Mo_2^{4+} complexes of **3** and **4**.

Reference:

(2) Snatzke, G. Circular Dichroism and Absolute Conformation: Application of Qualitative MO Theory to Chiroptical Phenomena. *Angew. Chem., Int. Ed.* **1979**, *18*: 363–377; *Angew. Chem.* **1979**, *91*: 380−393.

2.9 WST-8 cell viability assay

Cell viability was measured using a cell count kit 8 (CCK-8) assay (Dojindo Laboratories, Kumamoto, Japan) which is based on the conversion of a water-soluble tetrazolium salt, 2-(2-methoxy-4-nitrophenyl)-3-(4-nitrophenyl)-5-(2,4-disulfophenyl)-2*H*-tetrazolium, monosodium salt (WST-8), to a water-soluble formazan dye upon reduction by dehydrogenases in the presence of an electron carrier (3). In brief, 5×10^3 cells were cultured in flat-bottomed 96 well plates with a final volume of 100 μL/well of culture medium. After 24 h, the cells were treated with different concentrations (3.2-320 mM) of each compounds (fusarins G1-G4) or DMSO for 48 h. CCK-8 solution (10 μL) was added to each well, followed by incubation for 2 h at 37 °C. Then, the plate was shaked thoroughly for 1 min. The absorbance of samples at 450 nm was measured using a microtiter plate reader (Sunrise Remote/Touch screen, Columbusplus, Austria). The growth rates as stimulated by the compounds were calculated by the following formula: $[(A_{compound}-A_{DMSO})/A_{DMSO}] \times 100\%$.

Fusarins G1–G4 (**1**–**4**) showed no effect on the proliferation of the HepG2 cell line, but stimulated the growth of the LO2 cell line after exposure at 3.2-320 mM (Figure S5).

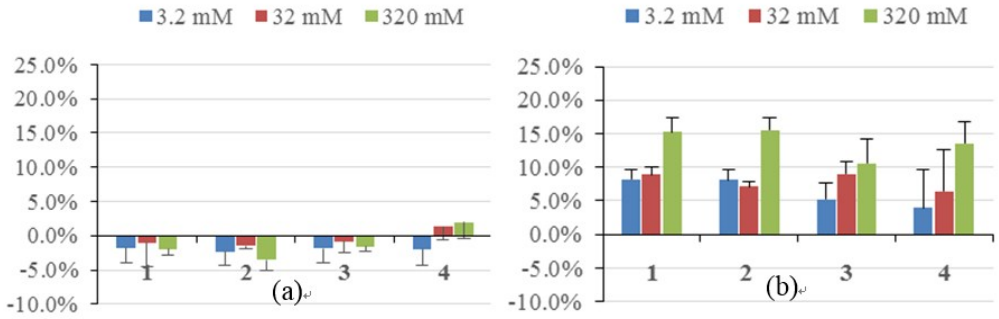

Figure S5. (a) Percentage of stimulated growth of HepG2 cells after exposure to 3.2-320 mM **1**–**4**; (b) Percentage of stimulated growth of LO2 cells after exposure to 3.2-320 mM **1**–**4**

Reference:

(3) Ishiyama, M.; Tominaga, H.; Shiga, M.; Sasamoto, K.; Ohkura, Y.; Ueno, K. A combined assay of cell viability and in vitro cytotoxicity with a highly water-soluble tetrazolium salt, neutral red and crystal violet. *Biol. Pharm. Bull.* **1996**, *19*: 1518–1520.

3. 1D, 2D NMR spectra of 1-5

3.1 The 1D, 2D NMR spectra of fusarin G1 (1)

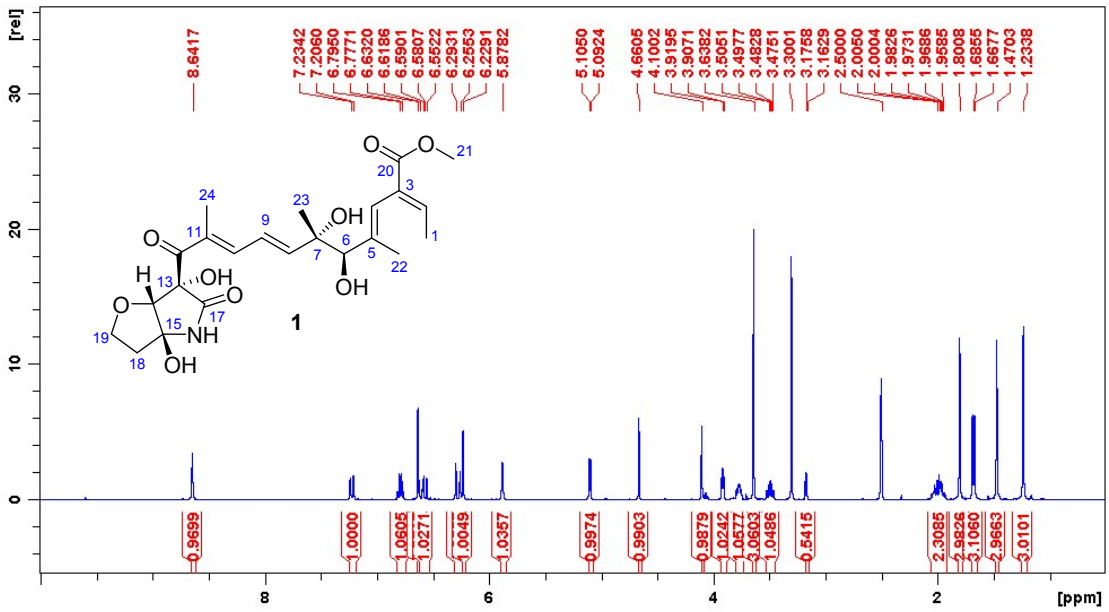

Figure S6. ^{1}H NMR spectrum of fusarin G1 (**1**) (400 MHz, in DMSO-d_6)

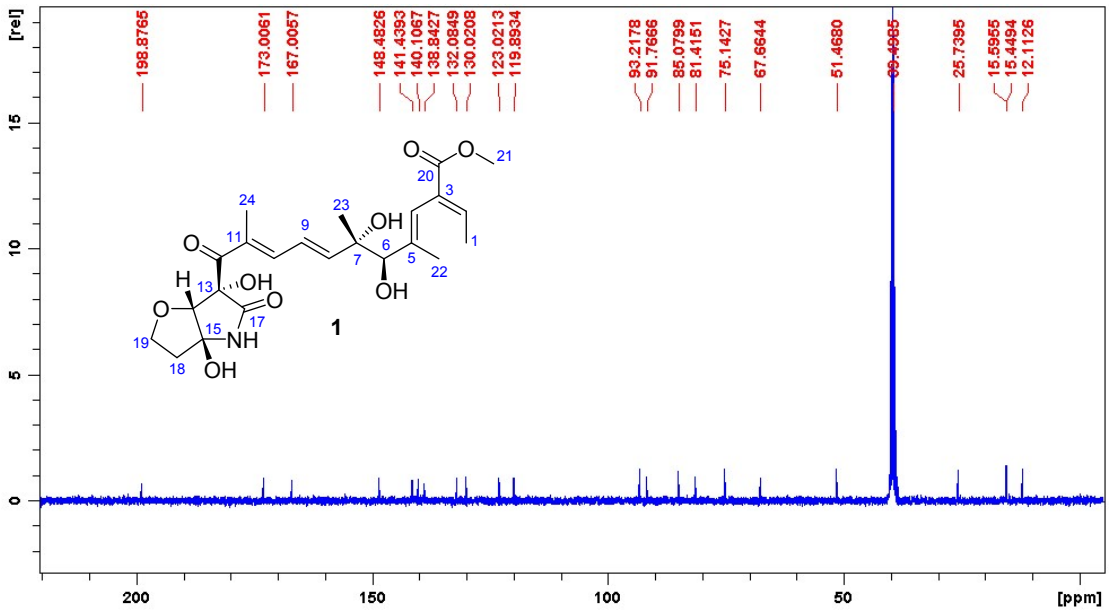

Figure S7. ^{13}C NMR spectrum of fusarin G1 (**1**) (100 MHz, in DMSO-d_6)

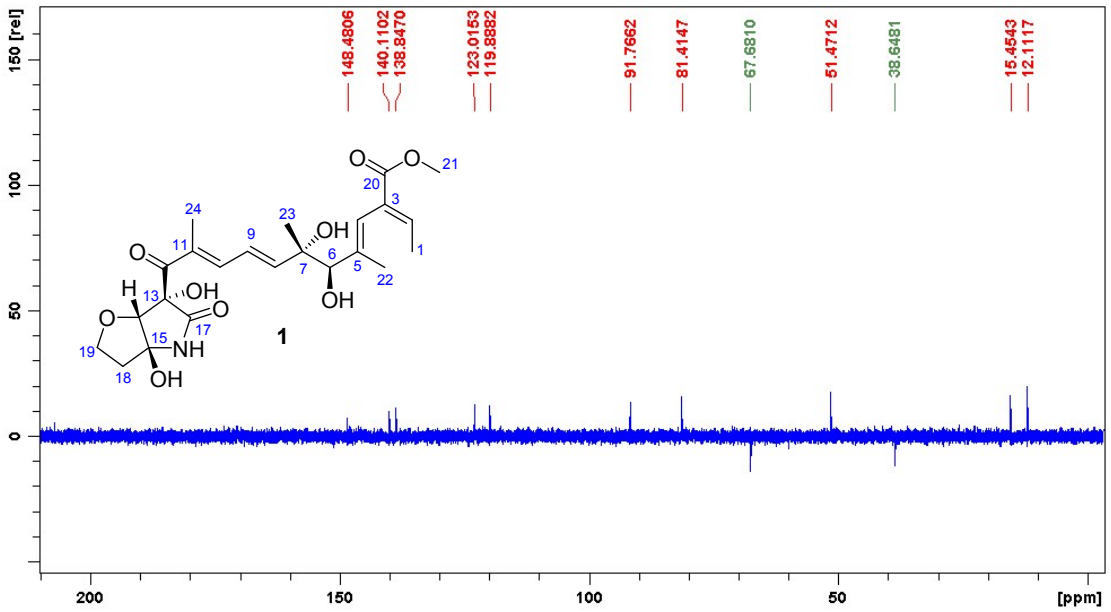

Figure S8. DEPT135 spectrum of fusarin G1 (**1**) (100 MHz, in DMSO-d_6)

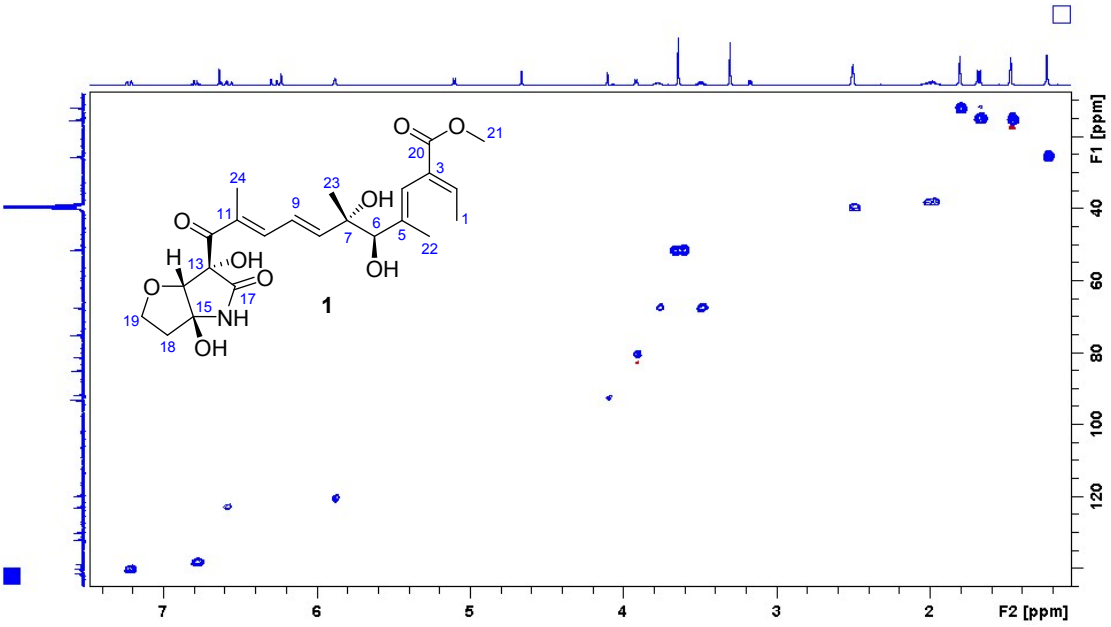

Figure S9. HSQC spectrum of fusarin G1 (**1**) (DMSO-d_6)

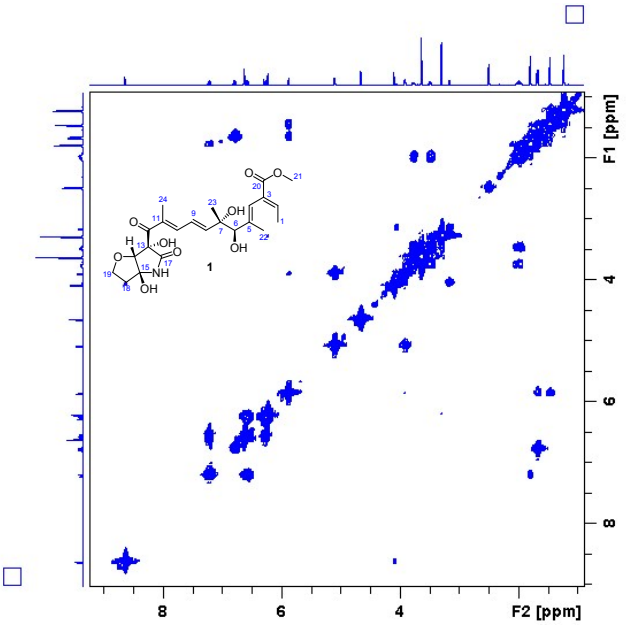

Figure S10. ^{1}H, ^{1}H-COSY spectrum of fusarin G1 (**1**) (DMSO-d_6)

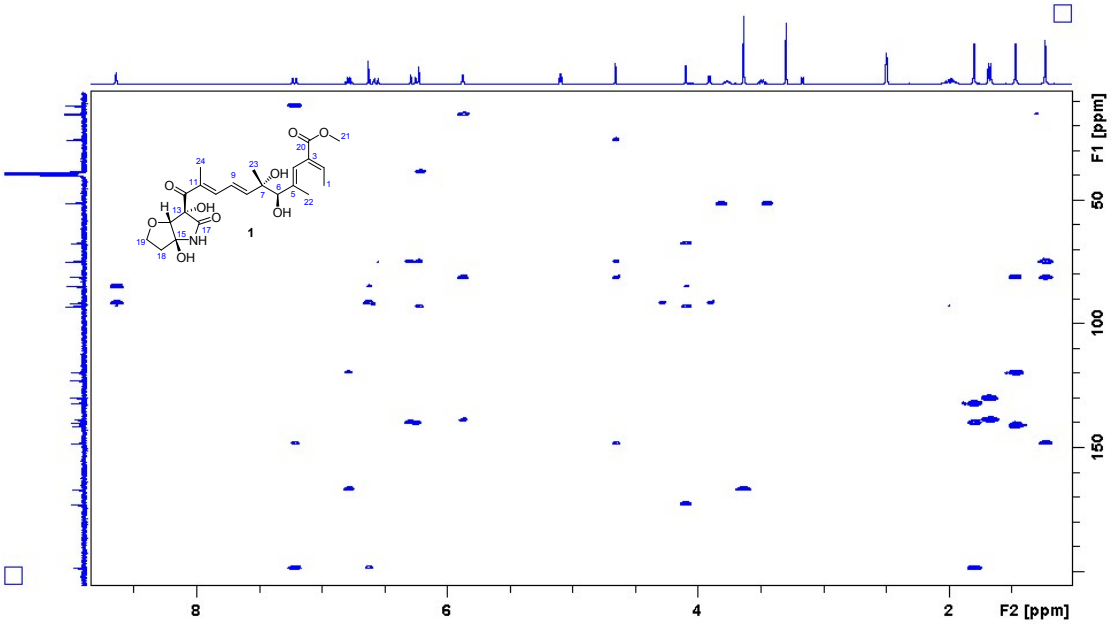

Figure S11. HMBC spectrum of fusarin G1 (**1**) (DMSO-d_6)

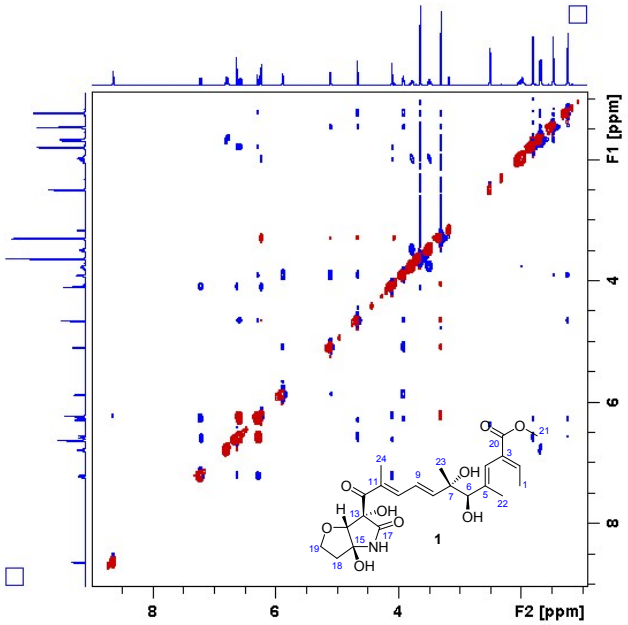

Figure S12. ROESY spectrum of fusarin G1 (**1**) (DMSO-d_6)

3.2 The 1D, 2D NMR spectra of fusarin G2 (2)

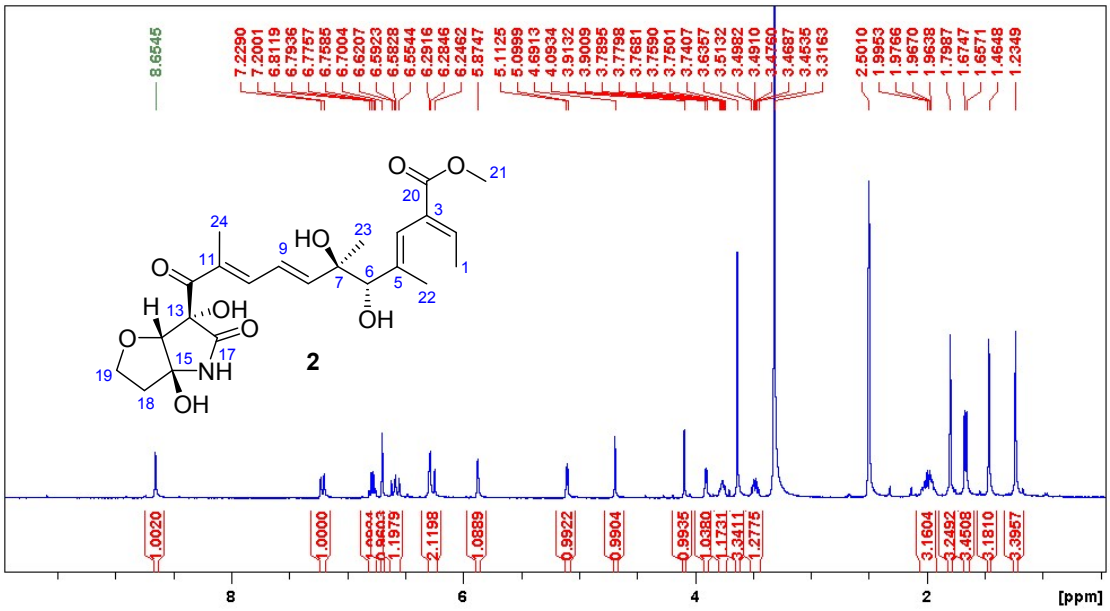

Figure S13. ^{1}H NMR spectrum of fusarin G2 (**2**) (400 MHz, in DMSO-d_6)

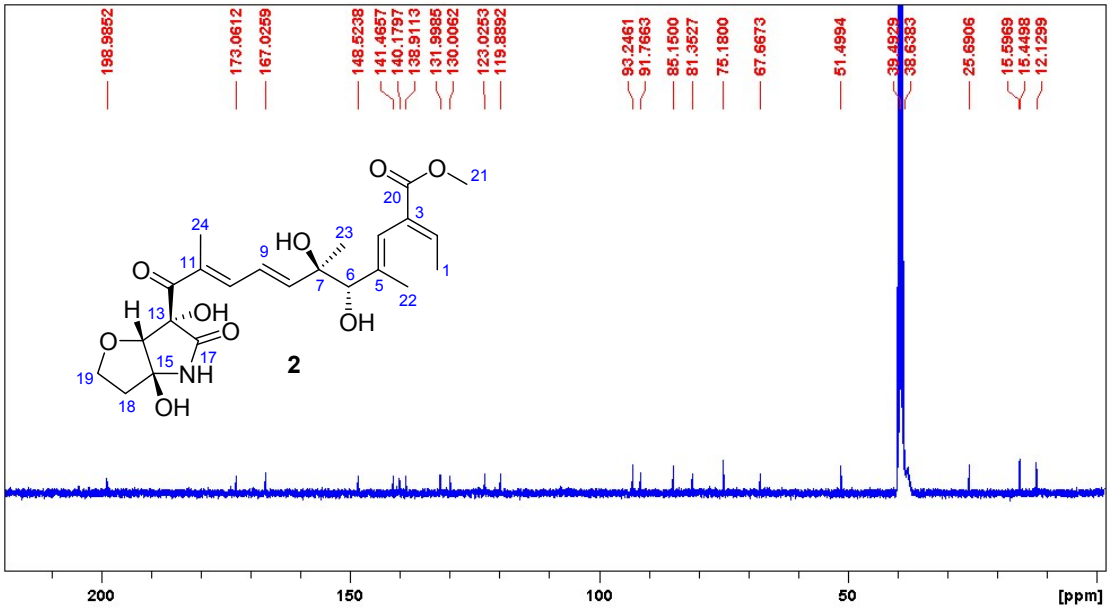

Figure S14. ^{13}C NMR spectrum of fusarin G2 (**2**) (100 MHz, in DMSO-d_6)

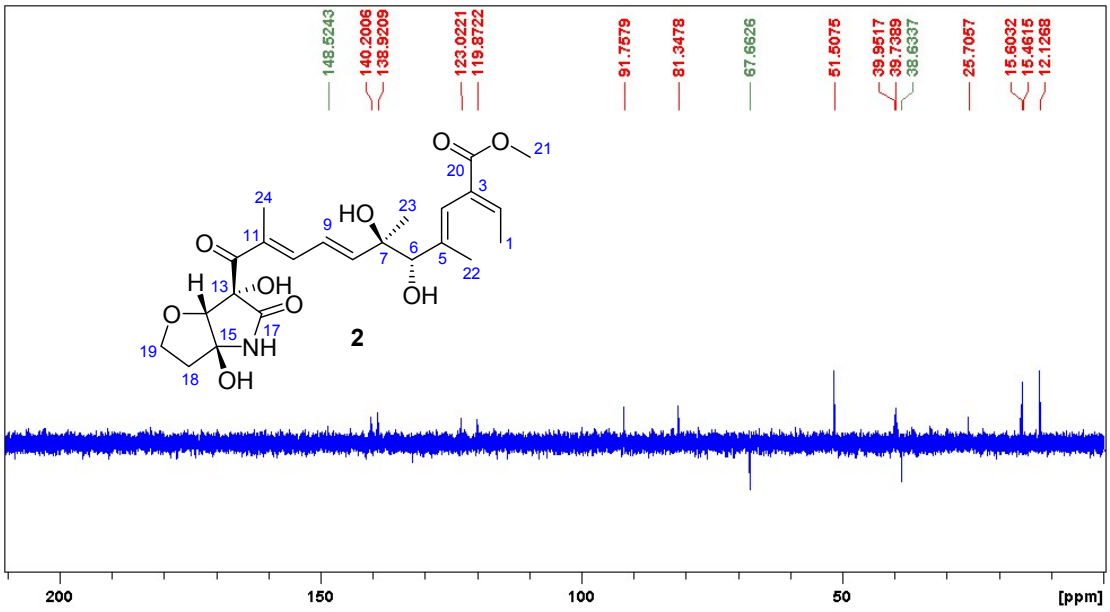

Figure S15. DEPT135 spectrum of fusarin G2 (**2**) (100 MHz, in DMSO-d_6)

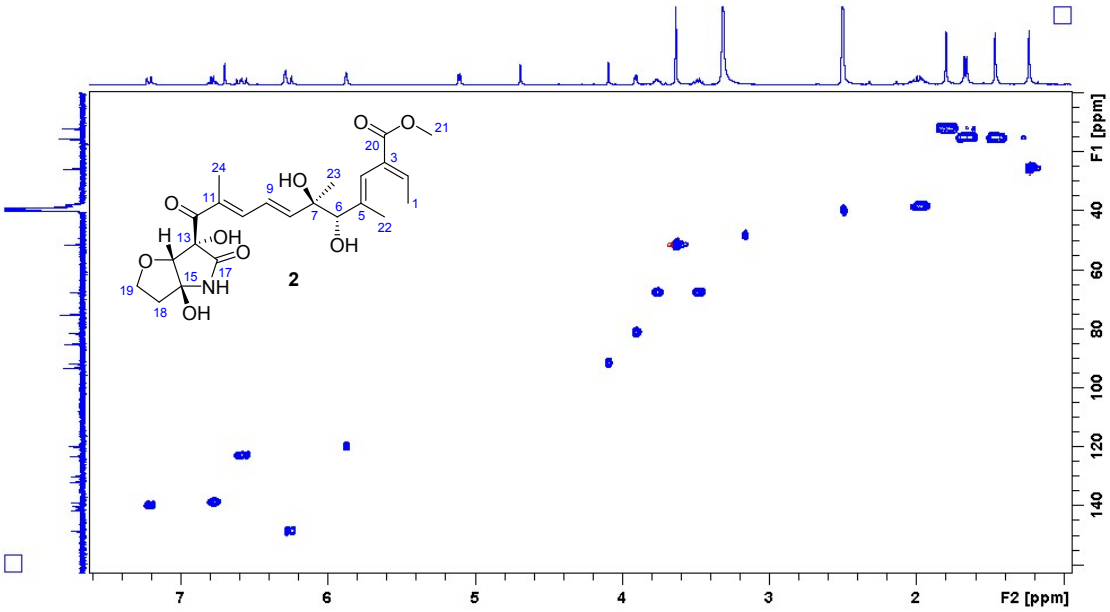

Figure S16. HSQC spectrum of fusarin G2 (**2**) (DMSO-d_6)

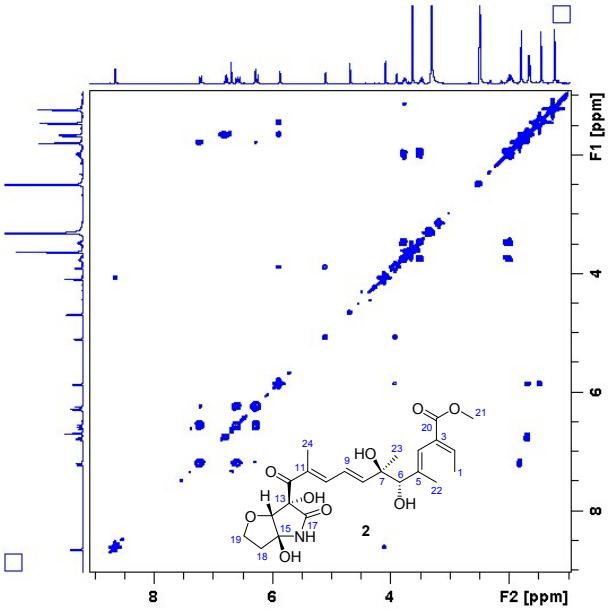

Figure S17. ^{1}H, ^{1}H-COSY spectrum of fusarin G2 (**2**) (DMSO-d_6)

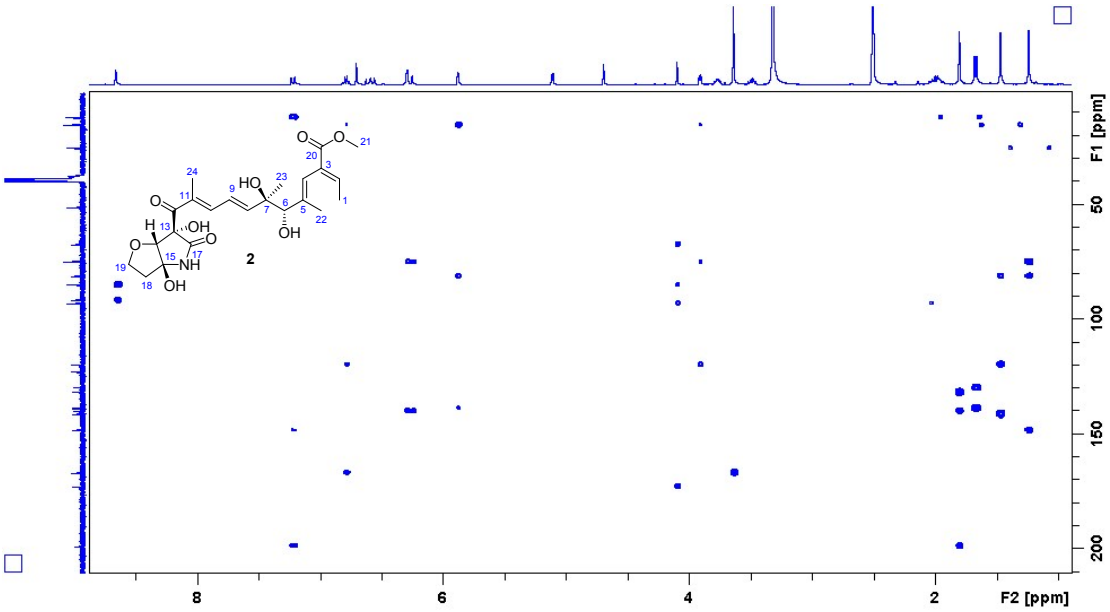

Figure S18. HMBC spectrum of fusarin G2 (**2**) (DMSO-d_6)

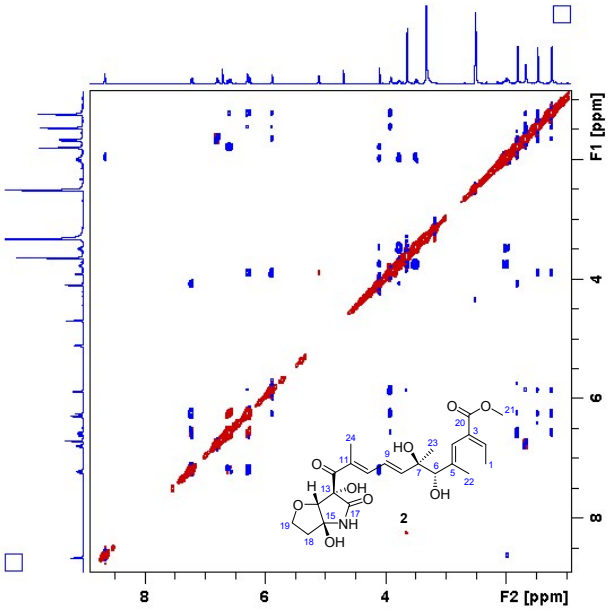

Figure S19. ROESY spectrum of fusarin G2 (**2**) (DMSO-d_6)

3.3 The 1D, 2D NMR spectra of fusarin G3 (3)

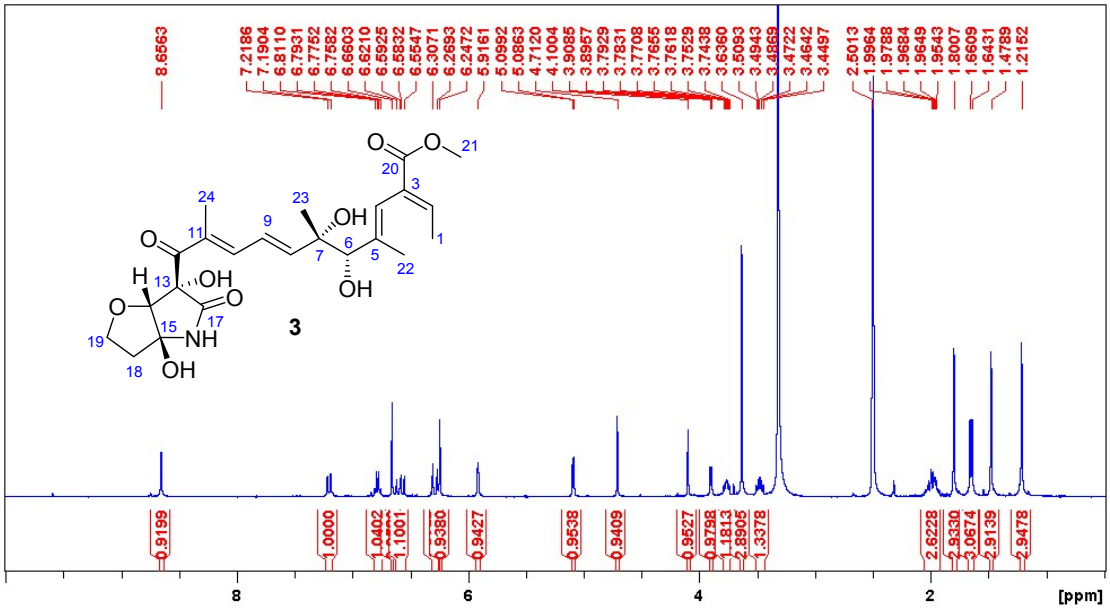

Figure S20. ^{1}H NMR spectrum of fusarin G3 (**3**) (400 MHz, in DMSO-d_6)

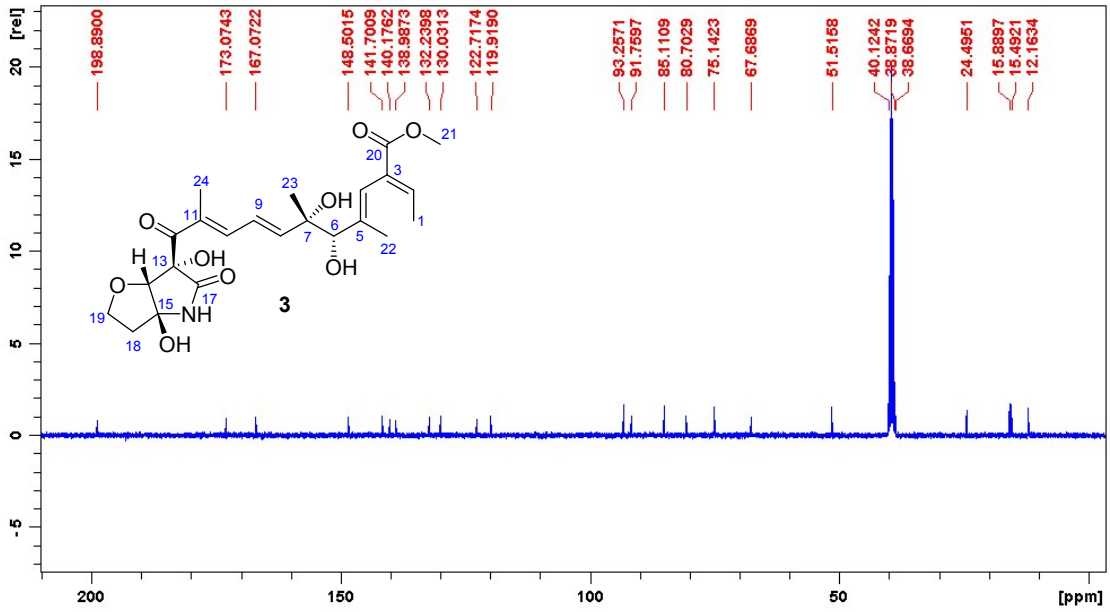

Figure S21. ^{13}C NMR spectrum of fusarin G3 (**3**) (100 MHz, in DMSO-d_6)

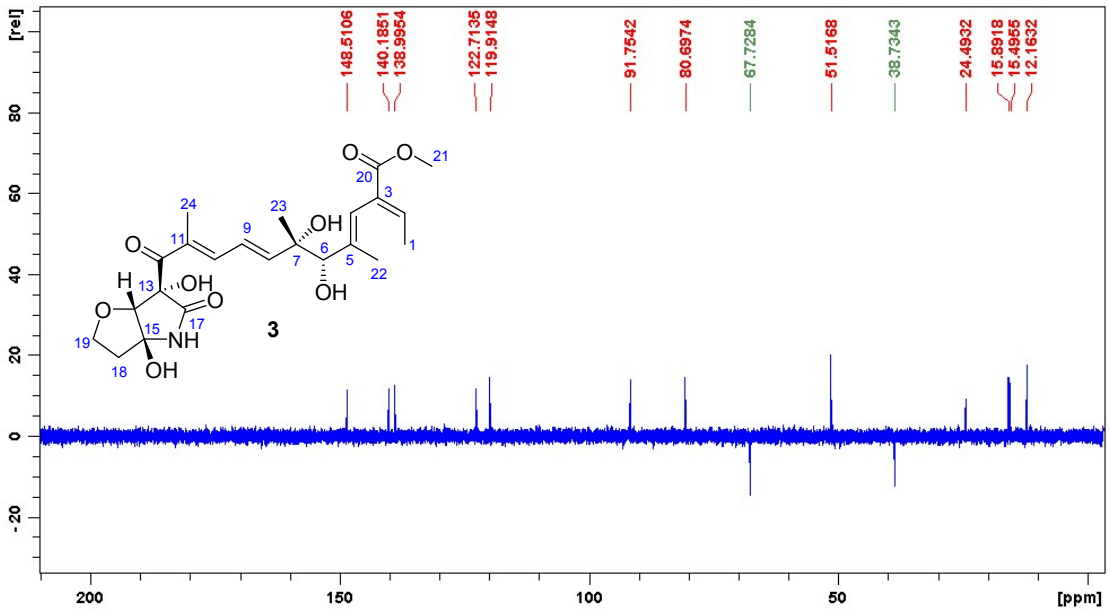

Figure S22. DEPT135 spectrum of fusarin G3 (**3**) (100 MHz, in DMSO-d_6)

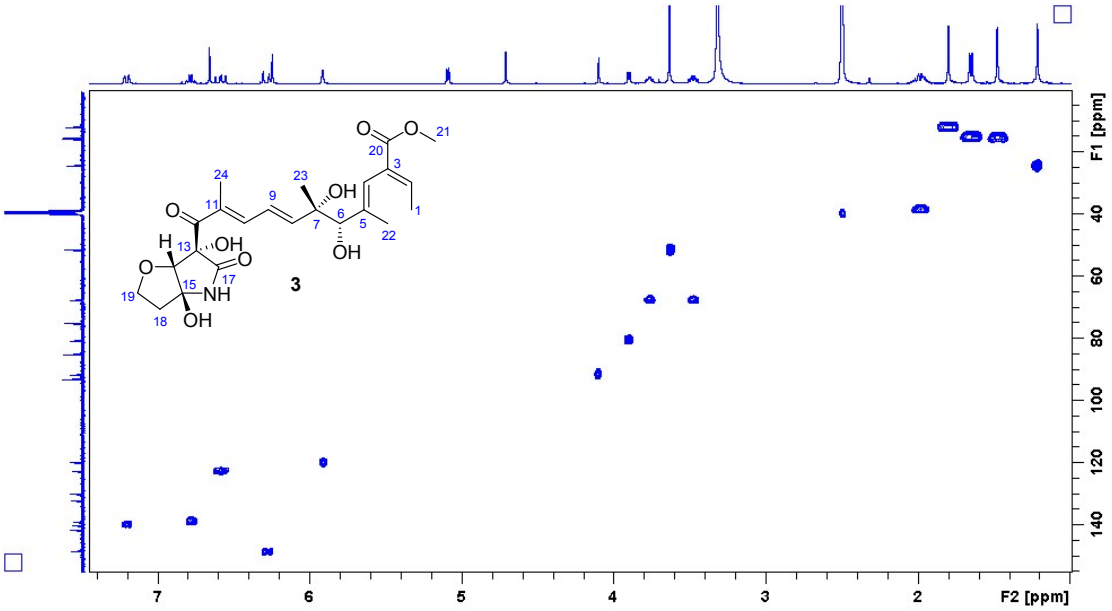

Figure S23. HSQC spectrum of fusarin G3 (**3**) (DMSO-d_6)

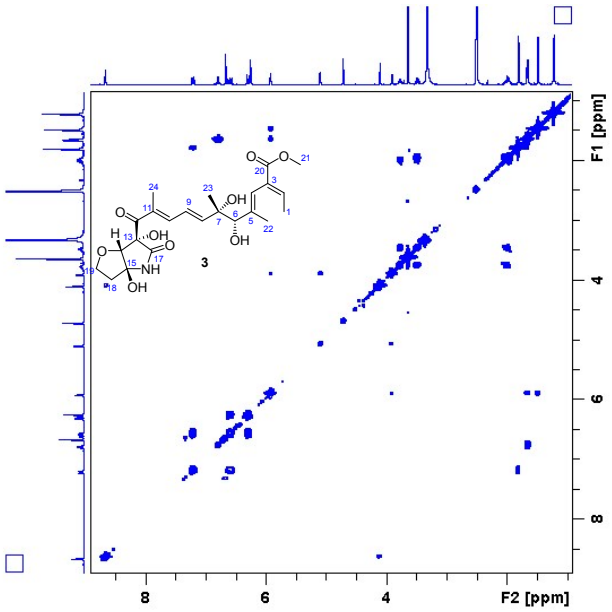

Figure S24. ^{1}H, ^{1}H-COSY spectrum of fusarin G3 (**3**) (DMSO-d_6)

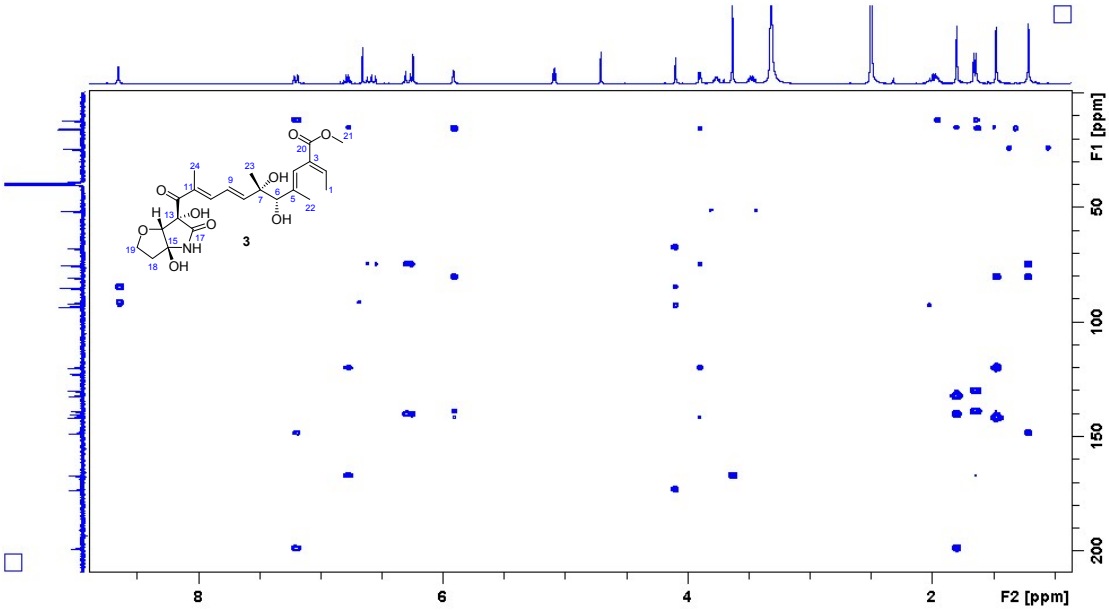

Figure S25. HMBC spectrum of fusarin G3 (**3**) (DMSO-d_6)

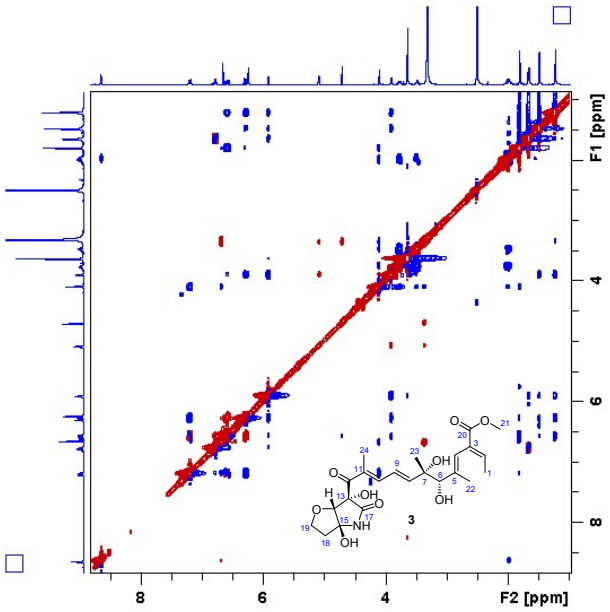

Figure S26. ROESY spectrum of fusarin G3 (**3**) (DMSO-d_6)

3.4 The 1D, 2D NMR spectra of fusarin G4 (4)

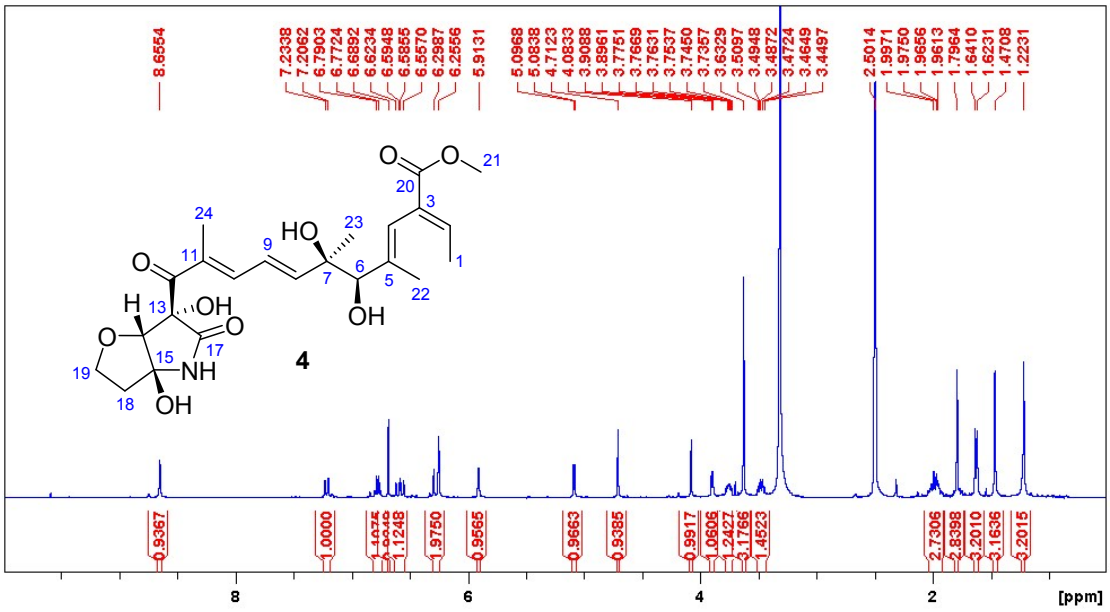

Figure S27. ^{1}H NMR spectrum of fusarin G4 (**4**) (400 MHz, in DMSO-d_6)

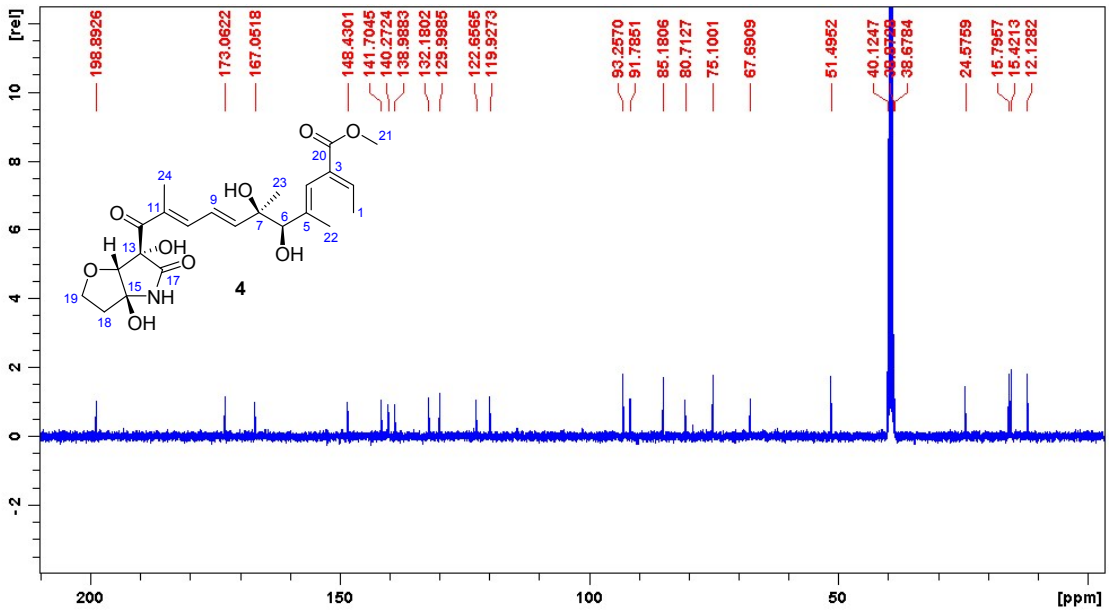

Figure S28. ^{13}C NMR spectrum of fusarin G4 (**4**) (100 MHz, in DMSO-d_6)

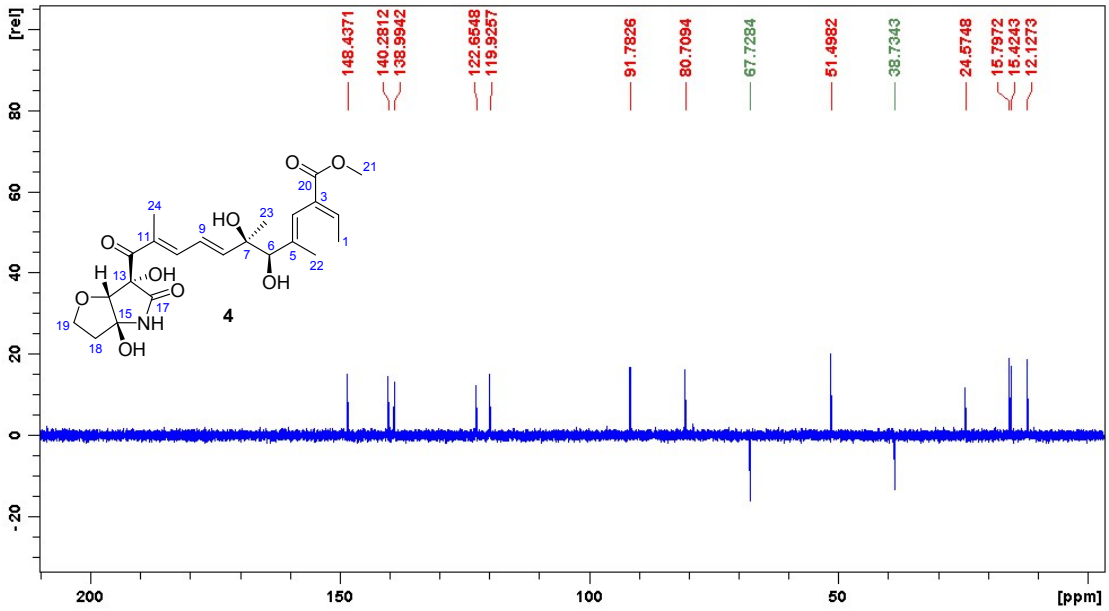

Figure S29. DEPT135 spectrum of fusarin G4 (**4**) (100 MHz, in DMSO-d_6)

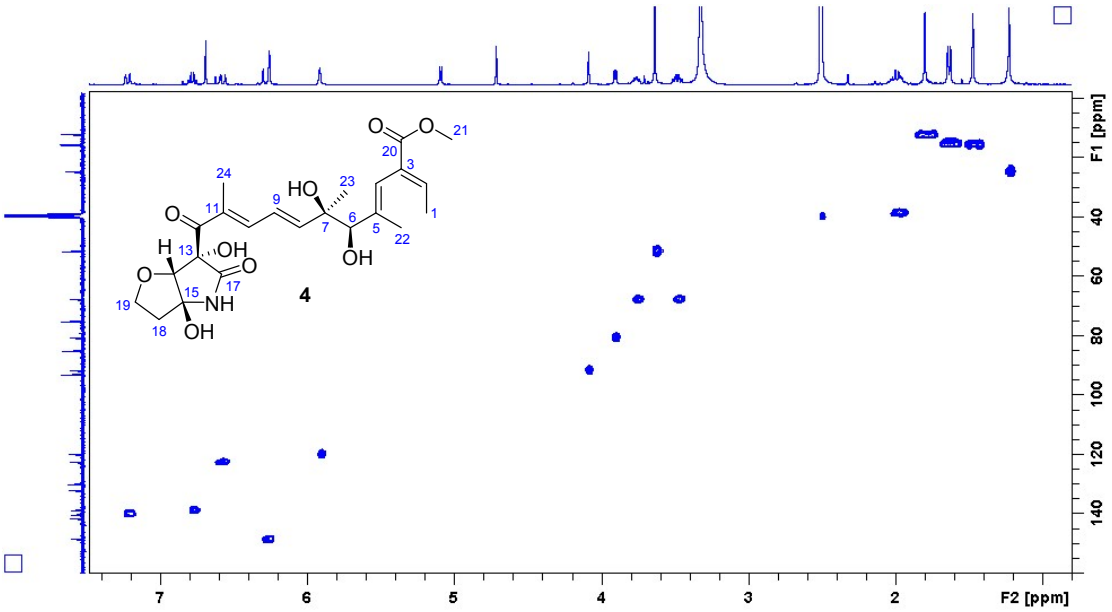

Figure S30. HSQC spectrum of fusarin G4 (**4**) (DMSO-d_6)

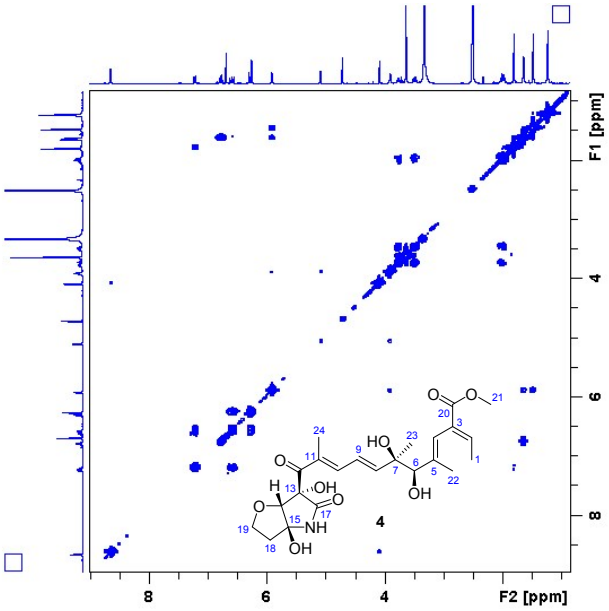

Figure S31. ^{1}H, ^{1}H-COSY spectrum of fusarin G4 (**4**) (DMSO-d_6)

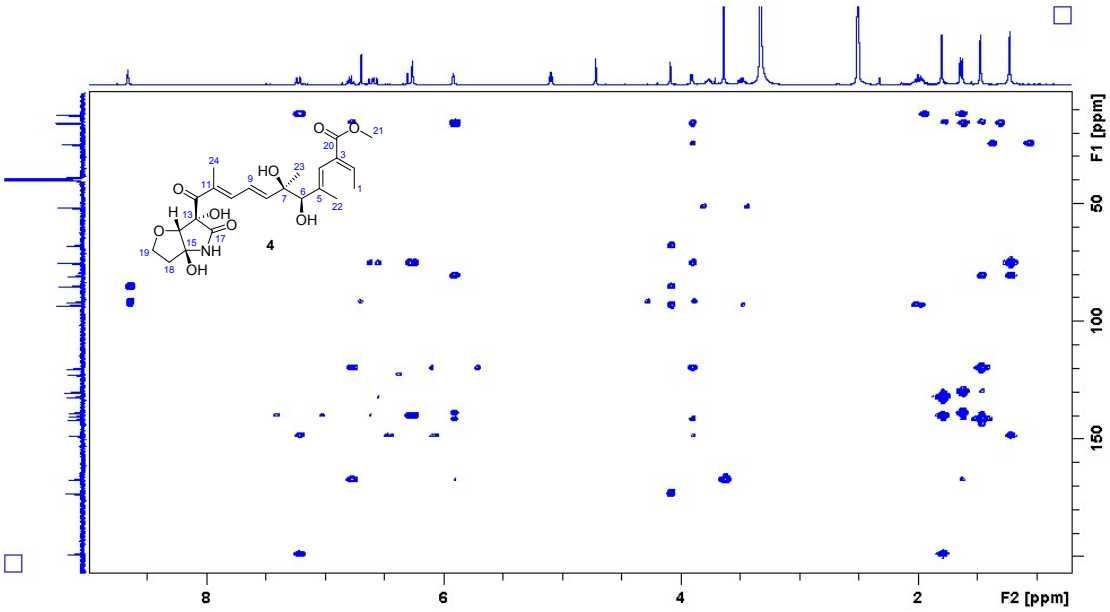

Figure S32. HMBC spectrum of fusarin G4 (**4**) (DMSO-d_6)

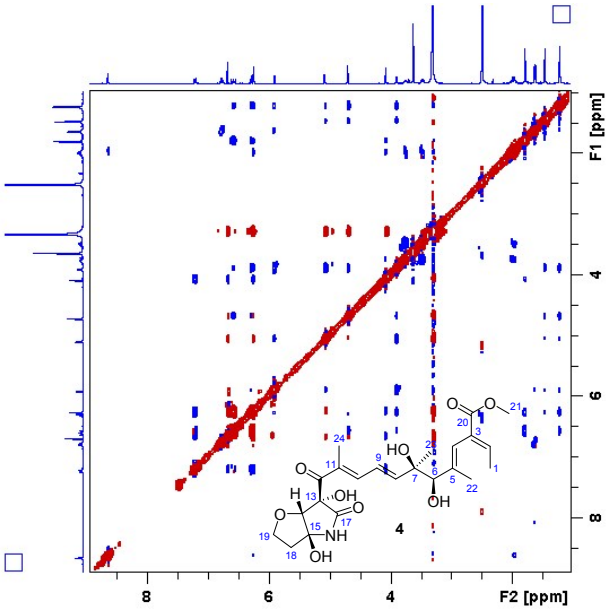

Figure S33. ROESY spectrum of fusarin G4 (**4**) (DMSO-d_6)

3.5 The 1D, 2D NMR spectra of 5

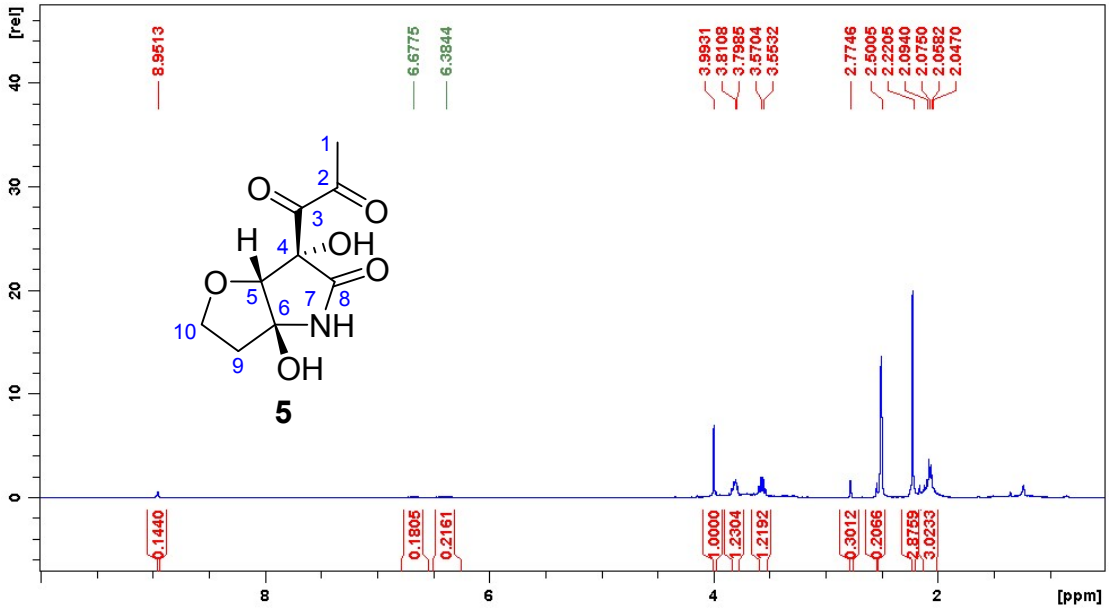

Figure S34. ^{1}H NMR spectrum of **5** (600 MHz, in DMSO-d_6)

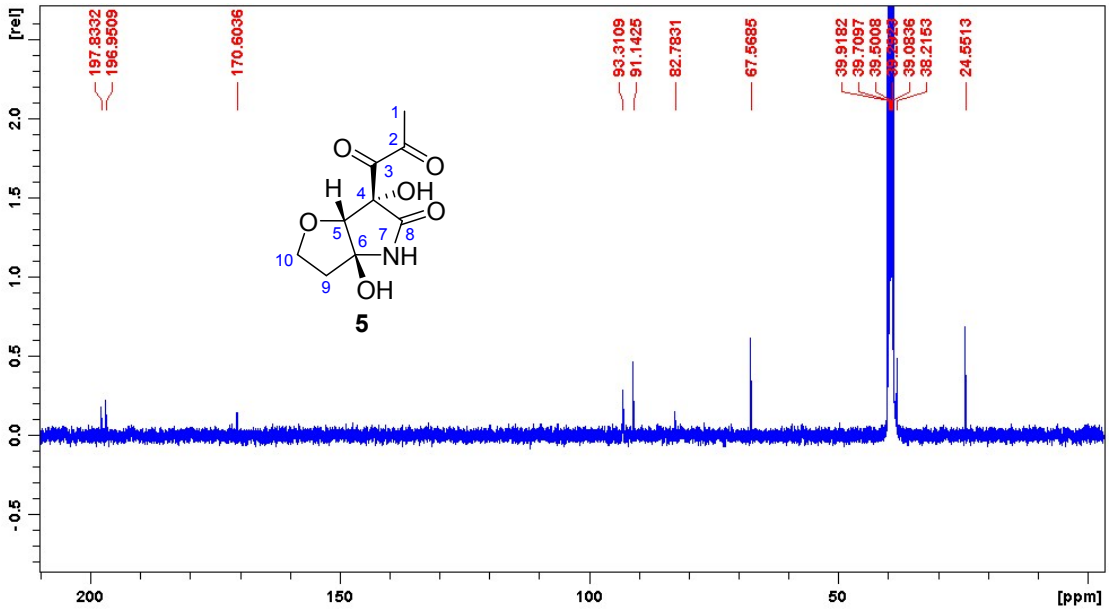

Figure S35. ^{13}C NMR spectrum of **5** (150 MHz, in DMSO-d_6)

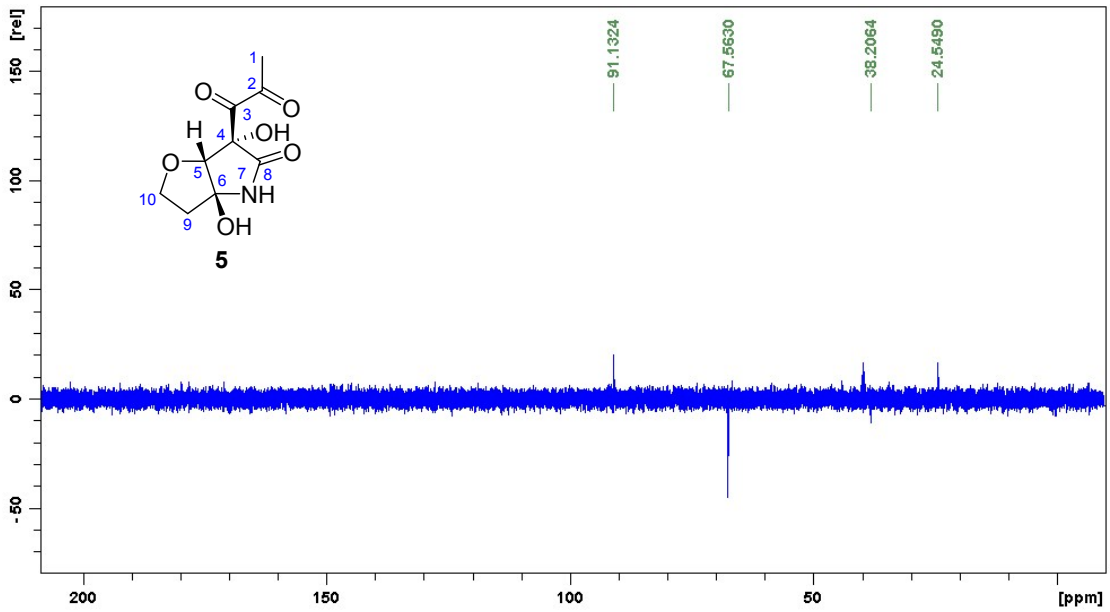

Figure S36. DEPT135 spectrum of **5** (150 MHz, in DMSO-d_6)

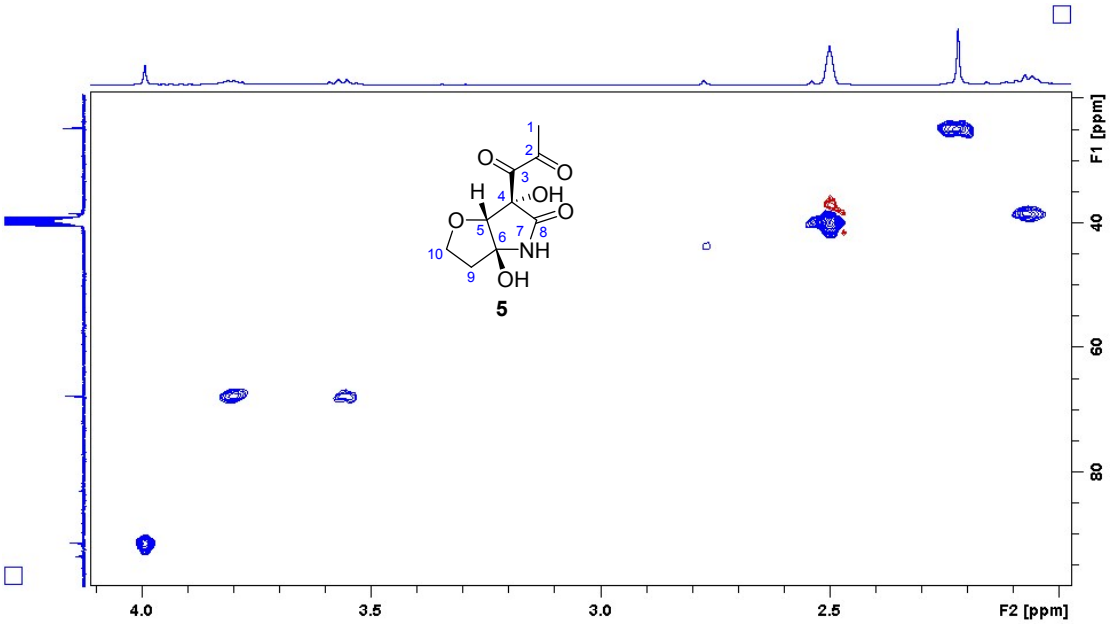

Figure S37. HSQC spectrum of **5** (DMSO-d_6)

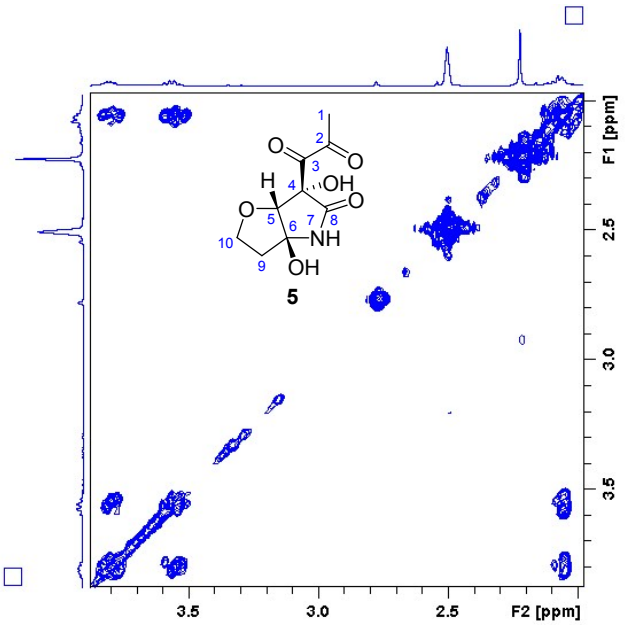

Figure S38. ^{1}H, ^{1}H-COSY spectrum of **5** (DMSO-d_6)

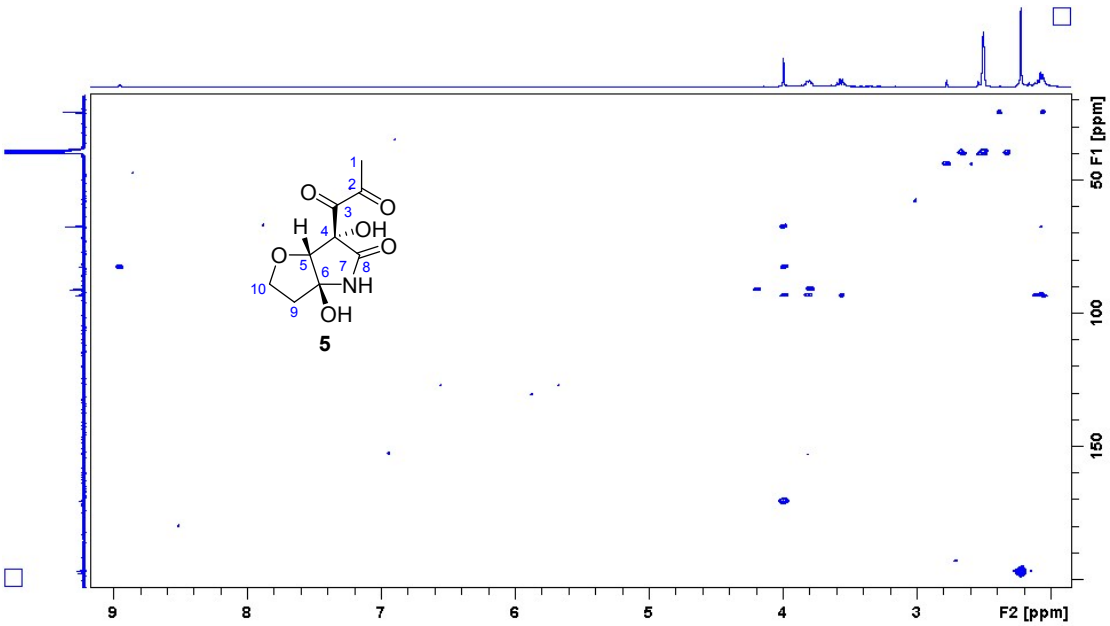

Figure S39. HMBC spectrum of **5** (DMSO-d_6)